Total-velocity-based finite volume discretization of two-phase Darcy flow in highly heterogeneous media with discontinuous capillary pressure

K. Brenner[1], J. Droniou[2], R. Masson[1], and E.H. Quenjel[1]

[1]University of Côte d'Azur, CNRS, Inria, LJAD, Parc Valrose 06108 Nice Cedex 02, France.
konstantin.brenner@univ-cotedazur.fr, roland.masson@univ-cotedazur.fr, quenjel@unice.fr.
[2]School of Mathematical Sciences, Monash University, Victoria, 3800, Australia. jerome.droniou@monash.edu.

February 25, 2021

Abstract

This work proposes a finite volume scheme for two-phase Darcy flow in heterogeneous porous media with different rock types. The fully implicit discretization is based on cell centered as well as face centered degrees of freedom in order to capture accurately the nonlinear transmission conditions at different rock type interfaces. These conditions play a major role in the flow dynamics. The scheme is formulated with natural physical unknowns, and the notion of global pressure is only introduced to analyse its stability and convergence. It combines a Two-Point Flux Approximation of the gradient normal fluxes with a Hybrid Upwinding approximation of the transport terms. The convergence of the scheme to a weak solution is established taking into account discontinuous capillary pressure at different rock type interfaces and the degeneracy of the phase mobilities. Numerical experiments show the additional robustness of the proposed discretization compared with the classical Phase Potential Upwinding approach.

1 Introduction

Two-phase flow in porous media plays a major role for understanding and predicting the behavior of subsurface flows. It is of crucial interest for many industrial and engineering applications including management of geothermal energy, enhanced oil recovery, CO2 sequestration and geological storage [4, 32]. The governing equations and constitutive laws of the flow lead to a complex system of partial differential equations [13, 37] accounting for the interaction between viscous, buoyancy and capillary forces. More importantly, contrasts in capillary forces at interfaces between different rock types have a strong impact on the flow paths of the fluids [34, 44]. This raises significant challenges in the development and mathematical analysis of accurate and efficient numerical methods.

This work focuses on the difficulties raised by the heterogeneity of the porous medium with different rock types. The main issue comes from the discontinuity in space of the capillary pressure function at different rock type interfaces modeled by strongly nonlinear transmission conditions. It is usually combined with large ranges of space and time scales induced by highly contrasted petrophysical properties. These characteristics challenge both the design of efficient numerical methods and their mathematical analysis. A typical example is the capillary barrier effect [7, 33, 43] which plays a chief role in oil migration in sedimentary basins, or flows in fractured porous media typically based on Discrete Fracture Matrix models [5, 8, 10, 29, 41].

Several numerical methods have been developed and analyzed for the discretization of two-phase Darcy flow in heterogeneous porous media. Let us refer for example to [14, 15, 27, 39, 17] in the case of a spatially homogeneous capillary pressure function. The case of discontinuous capillary pressures is investigated in [23] using a Discontinuous Galerkin (DG) discretization and developed in [34] based on a Mixed Finite Element (MFE) discretization. A space-time domain decomposition method using the optimized Schwarz waveform relaxation algorithm has been proposed in [2] for a purely capillary diffusive two-phase flow model. The convergence of a Two Point Flux Approximation (TPFA) scheme for a simplified model was the object of the work [21]. Assuming the non-degeneracy of the mobilities, a gradient discretization [19], including various conforming and non-conforming methods, was conceived and analyzed in [26] for an incompressible two-phase flow problem in heterogeneous porous media. This gradient discretization was extended to the case of hybrid dimensional two-phase Darcy flows in fractured porous media in [20]. Based on the global pressure formulation for the viscous forces and on the Kirchhoff transform for the capillary diffusion, a Two-Point Flux Approximation (TPFA) finite volume discretization was proposed and investigated in [7]. This is to our knowledge the only work to derive a convergence analysis of a fully coupled two-phase Darcy flow model accounting both for discontinuous capillary pressure and for the degeneracy of the phase mobilities.

The global pressure is a key mathematical tool to circumvent the fact that the phase pressure is not controlled in zones where the phase mobility vanishes. On the other hand, it is physically meaningless and not practical from the numerical point of view. It results that practical discretizations are based on natural variables like the phase pressures, the capillary pressure and the saturations. Likewise, the Kirchhoff transform is not easy to implement and rarely used in realistic applications.

The main objective of this work is to design a TPFA discretization based on natural variables and for which the convergence of the scheme can be achieved, taking into account discontinuous capillary pressure and the degeneracy of the mobilities. To capture the transmission conditions accurately at different rock type interfaces, the proposed scheme should include face unknowns at least at heterogeneous rock type interfaces. The time discretization should also be fully coupled and fully implicit to account for the strong coupling of the phase pressures and saturations at different rock type interfaces and to avoid severe restrictions on the time steps in highly permeable regions.

Our approach is based on the total velocity formulation of two-phase Darcy flow for which the model is expressed as an elliptic equation for the pressure coupled to a degenerate parabolic equation for the saturation. Both equations are weakly coupled in homogeneous regions but remain strongly nonlinearly coupled by the transmission conditions at interfaces between different rock types. Then, the discretization combines a two-point approximation (TPFA) of the gradient fluxes with a Hybrid Upwinding (HU) of the transport terms in the saturation equation. The HU transport scheme has been introduced in [25, 28] as an alternative to the Phase Potential Upwind (PPU) scheme [6, 37, 22, 1] for the approximation of the fractional flow, buoyancy and capillary terms in the saturation equation. In the framework of TPFA, it has been recently shown in [30, 31, 3] to provide additional nonlinear convergence robustness thanks to better smoothness properties of the HU two-point monotone fluxes compared with the PPU fluxes. A fully implicit Vertex Approximate Gradient (VAG) discretization combined with the HU scheme has been introduced recently in [10] also showing a better robustness than the VAG PPU version.

A crucial feature of the discretization proposed in this work relies on a specific approximation of the phase mobilities in the expression of the discrete total velocity. Contrary to the discretization of [7], this choice allows to relate the phase pressure expression of the total velocity with the global pressure and consequently to recover the control of the global pressure in the energy estimates.

A second objective of this work is to compare the proposed TPFA HU discretization in terms of accuracy and efficiency with the more classical TPFA PPU discretization. The comparison includes the use of face unknowns either at all interior faces or alternatively only at interfaces between different rock types. Moreover we will also investigate different strategies to solve the fully coupled nonlinear system at each time step of the simulation either based on a local non-linear interface solver or on a regularization of the non-wetting phase flux continuity equation at the interfaces.

The rest of this paper is outlined now. Section 2 introduces the mathematical model governing the two-phase Darcy flow in heterogeneous porous media in total velocity formulation. A special attention is placed on the formulation of the nonlinear transmission conditions between different rock types. In Section 3, our fully implicit TPFA HU discretization is detailed based on a classical upwind approximation of the fractional flow as well as on a monotone approximation of the capillary flux. The centered approximation of the phase mobilities in the total velocity plays a crucial role to recover the control on the global pressure in the energy estimates. The existence of a solution is obtained by a topological degree argument exploiting the energy estimates and the L^∞ bound on the capillary pressure. In Section 4, the convergence of the discrete solution to a weak solution is established up to a subsequence. The proof relies on the relative compactness of the discrete saturations using a discrete Aubin Simon theorem. The transmission conditions are proved to be satisfied by the limit by establishing the convergence of the discrete traces at different rock type interfaces. Compared with [7], a new proof is provided based on the boundedness of the capillary pressure as well as a key decomposition of the non-linearities accounting for the transmission conditions. In the numerical section (Section 5) our TPFA HU discretization is compared to the TPFA PPU scheme in terms of both accuracy and efficiency on two test cases. The first one is the simulation of oil migration in a one dimensional basin with a drain and a capillary barrier. The second test case considers the oil migration in a 2D Discrete Fracture Matrix model incorporating a complex network of fractures and highly heterogeneous matrix fracture petrophysical and hydrodynamical properties.

2 Mathematical problem

Let Ω be a bounded polyhedral domain of $\mathbb{R}^d$ ($d \in \mathbb{N}$, $d \geq 2$). The domain Ω is assumed to be split into two polyhedral subdomains Ω_i, $i \in \{1, 2\}$, each having its own rock type i, such that $\overline{\Omega} = \overline{\Omega}_1 \cup \overline{\Omega}_2$, $\Omega_1 \cap \Omega_2 = \emptyset$. The interface $\partial\Omega_1 \cap \partial\Omega_2$ between the two-subdomains is denoted by Γ. Let $(0, t_f)$ denote the time interval with $t_f > 0$ and let us consider an immiscible and incompressible two-phase Darcy flow with $\{\mathrm{w}, \mathrm{nw}\}$ the set of wetting and non-wetting phases. Denoting by p_i^α, $\alpha \in \{\mathrm{w}, \mathrm{nw}\}$, the phase pressures and by π_i the capillary pressure, the mathematical formulation of the model is defined by the volume conservation of each phase α in each subdomain $i \in \{1, 2\}$

$$\phi(\mathbf{x})\partial_t s_i^\alpha(\pi_i) + \nabla \cdot \mathbf{V}_i^\alpha = 0, \quad \text{in} \quad Q_{t_f}^i = \Omega_i \times (0, t_f), \tag{2.1}$$

together with the capillary relation

$$\pi_i = p_i^{\mathrm{nw}} - p_i^{\mathrm{w}}. \tag{2.2}$$

In (2.1), ϕ is the porous medium porosity depending on $\mathbf{x} \in \Omega$, s_i^α is the saturation of the phase α as a function of the capillary pressure π_i such that $s_i^{\mathrm{nw}} + s_i^{\mathrm{w}} = 1$, and $\mathbf{V}_i^\alpha$ is the velocity of phase α defined by the generalized Darcy law

$$\mathbf{V}_i^\alpha = -\frac{k_{r,i}^\alpha(s_i^\alpha(\pi_i))}{\mu^\alpha}\Lambda(\mathbf{x})(\nabla p_i^\alpha - \rho^\alpha \mathbf{g}). \tag{2.3}$$

In (2.3), $k_{r,i}^\alpha$ is the phase relative permeability as a function of the phase saturation, μ^α is the constant dynamic viscosity of phase α, and Λ denotes the intrinsic permeability as a function of $\mathbf{x} \in \Omega$. The vector $\mathbf{g} \in \mathbb{R}^d$ is the gravity acceleration vector.

The system (2.1)-(2.2) involves strong nonlinear couplings and degenerates when switching from unsaturated to saturated zones. Besides, the constitutive laws and physical parameters can vary strongly with respect to space across the interface Γ, which implies highly nonlinear transmission conditions specified below and plays a key role in the flow dynamics. These issues challenge the design of efficient numerical schemes. Our approach is based on the total velocity formulation, which, roughly speaking, weakly decouples the system into a degenerate parabolic equation for the non-wetting phase saturation and an elliptic equation for the non-wetting phase pressure. To simplify the presentation, the gravity term is neglected in the remaining description of the model and of the numerical scheme although it will be considered in the numerical tests. For convenience, let us denote the non-wetting phase saturation function by $s_i = s_i^{\mathrm{nw}}$ and let us define the phase mobilities by

$$M_i^\alpha(s) = \begin{cases} \dfrac{k_{r,i}^{\mathrm{nw}}(s)}{\mu^{\mathrm{nw}}} & \text{for } \alpha = \mathrm{nw}, \\ \dfrac{k_{r,i}^{\mathrm{w}}(1-s)}{\mu^{\mathrm{w}}} & \text{for } \alpha = \mathrm{w}, \end{cases}$$

as functions of the non-wetting phase saturation. The total velocity is defined as the sum of the phase velocities such that

$$\mathbf{V}_i^T = \sum_{\alpha\in\{\mathrm{nw},\mathrm{w}\}} \mathbf{V}_i^\alpha = - \sum_{\alpha\in\{\mathrm{nw},\mathrm{w}\}} M_i^\alpha(s_i(\pi_i))\Lambda(\mathbf{x})\nabla p_i^\alpha.$$

The total mobility and the phase fractional flow are defined as functions of the non wetting-phase saturation by

$$M_i^T(s) = M_i^{\mathrm{nw}}(s) + M_i^{\mathrm{w}}(s), \quad f_i^\alpha(s) = \frac{M_i^\alpha(s)}{M_i^T(s)}.$$

Using these notations, the non-wetting phase velocity can be expressed by

$$\mathbf{V}_i^{\mathrm{nw}} = f_i^{\mathrm{nw}}(s_i(\pi_i))\mathbf{V}_i^T - \eta_i(s_i(\pi_i))\Lambda(\mathbf{x})\nabla\pi_i. \tag{2.4}$$

with

$$\eta_i(s) = \frac{M_i^{\mathrm{nw}}(s)M_i^{\mathrm{w}}(s)}{M_i^T(s)}.$$

Substituting (2.4) in the non-wetting phase saturation equation (2.1), the system (2.1)-(2.2)-(2.3) is equivalent to its total velocity formulation

$$\begin{cases} \phi(\mathbf{x})\partial_t s_i(\pi_i) + \nabla\cdot\Big(f_i^{\mathrm{nw}}(s_i(\pi_i))\mathbf{V}_i^T - \eta_i(s_i(\pi_i))\Lambda(\mathbf{x})\nabla\pi_i\Big) = 0, \\ \nabla\cdot\mathbf{V}_i^T = 0, \\ \mathbf{V}_i^T = - \displaystyle\sum_{\alpha\in\{\mathrm{nw},\mathrm{w}\}} M_i^\alpha(s_i(\pi_i))\Lambda(\mathbf{x})\nabla p_i^\alpha, \\ \pi_i = p_i^{\mathrm{nw}} - p_i^{\mathrm{w}}, \end{cases} \tag{2.5}$$

using the phase pressures and capillary pressure as primary unknowns. This system is complemented by the following no-flux boundary conditions

$$\begin{aligned} \Big(f_i^{\mathrm{nw}}(s_i(\pi_i))\mathbf{V}_i^T - \eta_i(s_i(\pi_i))\Lambda\nabla\pi_i\Big)\cdot\mathbf{n}_i &= 0 \quad \text{on } (\partial\Omega\cap\partial\Omega_i)\times(0,t_f), \\ \mathbf{V}_i^T\cdot\mathbf{n}_i &= 0 \quad \text{on } (\partial\Omega\cap\partial\Omega_i)\times(0,t_f), \end{aligned} \tag{2.6}$$

where $\mathbf{n}_i$ denotes the outward unit normal vector to $\partial\Omega\cap\partial\Omega_i$. The non-wetting phase pressure is determined up to a constant which is fixed by the following condition

$$\sum_{i\in\{1,2\}} \int_{\Omega_i} p_i^{\mathrm{nw}}(\mathbf{x},\cdot)\,\mathrm{d}\mathbf{x} = 0 \quad \text{on} \quad (0,t_f). \tag{2.7}$$

The initial condition prescribes that

$$\pi_{i_{|t=0}} = \pi_i^0 \quad \text{in} \quad \Omega_i. \tag{2.8}$$

The system (2.5) is the starting point of the discretization introduced in Section 3. However, the proper definition of a weak continuous solution to (2.5) requires the introduction of the global pressure and of the Kirchhoff transform as specified below.

Global pressure

Although the discretization will be based on the formulation (2.5) using the phase pressures and capillary pressure as primary unknowns, it is well known that, at the continuous level, the gradient of the phase pressure is not well defined on the regions where the phase mobility vanishes. Following [7], a possible way to define properly the phase pressures relies on the extension of the concept of global pressure to different rock types.

Let us define the artificial pressures

$$G_i^{\mathrm{nw}}(v) = \int_0^v f_i^{\mathrm{nw}}(s_i(u))\,\mathrm{d}u, \quad G_i^{\mathrm{w}}(v) = \int_0^v f_i^{\mathrm{w}}(s_i(u))\,\mathrm{d}u. \tag{2.9}$$

leading to define the global pressure in each subdomain by

$$P_i = p_i^{\mathrm{w}} + G_i^{\mathrm{nw}}(\pi_i) = p_i^{\mathrm{nw}} - G_i^{\mathrm{w}}(\pi_i), \quad i = 1, 2. \tag{2.10}$$

Note that the global pressure is not continuous at the interface between different rock types $i \in \{1, 2\}$. To check formally how the global pressure circumvent the difficulties raised by the degeneracy of the phase mobilities, let us write for $i \in \{1, 2\}$

$$\begin{aligned} M_i^T(s_i(\pi_i))\Lambda\nabla P_i &= M_i^{\mathrm{w}}(s_i(\pi_i))\Lambda(\nabla p_i^{\mathrm{w}} + \nabla G_i^{\mathrm{nw}}(\pi_i)) + M_i^{\mathrm{nw}}(s_i(\pi_i))\Lambda(\nabla p_i^{\mathrm{nw}} - \nabla G_i^{\mathrm{w}}(\pi_i)) \\ &= M_i^{\mathrm{w}}(s_i(\pi_i))\Lambda\nabla p_i^{\mathrm{w}} + M_i^{\mathrm{nw}}(s_i(\pi_i))\Lambda\nabla p_i^{\mathrm{nw}} \\ &= \mathbf{V}_i^T. \end{aligned}$$

Since the total mobility M_i^T does not vanish (see Assumption ($\mathbf{A}_3$)), we can control the global pressure P_i and define the total velocity. Note also that the trace of P_i at the interface Γ is well-defined which is a key point to define the transmission conditions at the interface below. We emphasize that the global pressure concept holds a strong and useful mathematical sense but it has no clear physical meaning and it is not convenient from the numerical point of view. For this reason, as opposed to the discretization proposed in [7], the numerical scheme will only involve physical meaningful quantities like the phase pressures, the capillary pressure and the total velocity. The global pressure will be only used as intermediate tool to perform the convergence analysis of the scheme.

Kirchhoff transforms

Similarly to the phase pressures, the gradient of the capillary pressure cannot be controlled due to the degeneracy of the function η_i at $s = 0$ and $s = 1$. This classically leads to the introduction of the Kirchhoff transform F_i defined by

$$F_i(\nu) = \int_0^\nu \eta_i(s_i(u))\,\mathrm{d}u,$$

such that, formally, $\eta_i(s_i(\pi_i))\nabla\pi_i = \nabla F_i(\pi_i)$; this expression shows that F_i is naturally controlled by the energy estimates coming from the scheme. As for the global pressure, the Kirchhoff transform F_i will not be used in the numerical discretization of the capillary diffusion term, that will be based only on the capillary pressure, but it is needed at the continuous level. A stronger control will actually be obtained from the numerical scheme leading to the introduction of the following second Kirchhoff transform

$$\xi_i(\nu) = \int_0^\nu \sqrt{\eta_i(s_i(u))}\,\mathrm{d}u.$$

Interface conditions

We now specify the transmission conditions at the interface Γ between both rock types. These transmission conditions are stated in [7] with primary unknowns defined in each subdomain by the non-wetting phase saturation and the global pressure. They are adapted here to our choice of the capillary pressure and global pressure as primary unknowns.

From [44, 21, 11, 12, 7], the behavior of the phases at the interface Γ is governed by the natural statement: if one of the phase fluxes across Γ does not vanish, then the pressure of the same phase must be continuous on this interface. Otherwise, the upwind mobility vanishes. As shown in [11, 12, 7], this amounts to claiming that there exists a capillary pressure π_Γ at the interface Γ that should satisfy the following requirements. First, it accounts for the continuity of the wetting phase pressure at the interface Γ

$$\gamma_1 P_1 - G_1^{\mathrm{nw}}(\pi_\Gamma) = \gamma_2 P_2 - G_2^{\mathrm{nw}}(\pi_\Gamma), \qquad \text{a.e. on } \Gamma \times (0, t_f), \tag{2.11}$$

where γ_i denotes the trace operator on each side i of Γ. By adding π_Γ to both sides of equation (2.11), it also yields the continuity of the non-wetting phase by virtue of (2.9)-(2.10).

Secondly, as we will see in Definition 2.1, the Kirchhoff function F_i is supposed to be regular enough so that its trace also exists. The jump of the two-sided Kirchhoff transform F_i (and hence of the two-sided non-wetting phase saturation) at the interface Γ is governed by the following continuity condition

$$F_i(\pi_\Gamma) = \gamma_i F_i(\pi_i), \qquad \text{a.e. on } \Gamma \times (0, t_f). \tag{2.12}$$

Note that both equations in (2.12) for $i = 1, 2$ are enforced with the same interface capillary pressure π_Γ, as illustrated in Figure 1.

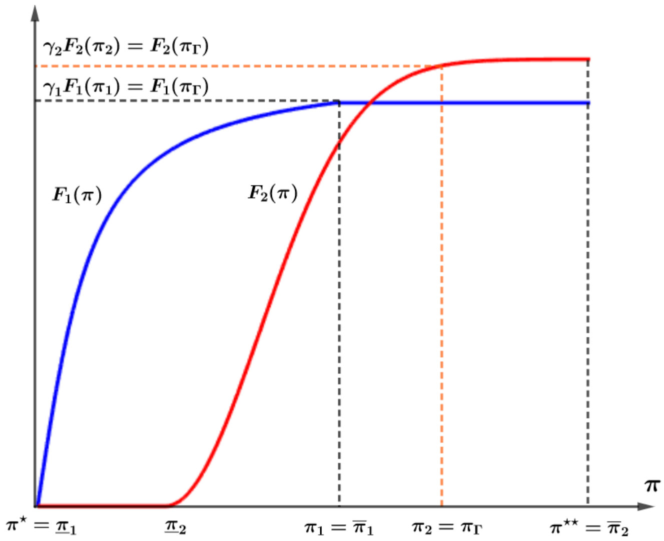

Figure 1: Example of Kirchhoff transforms $(F_i)_{i=1,2}$ for two rock types as functions of the capillary pressure π, and illustration of the continuity condition (2.12) for a given interface capillary pressure π_Γ and given subdomain capillary pressure solutions π_i.

Additionally, the continuity of the normal non-wetting phase and total velocities

$$\begin{aligned} \sum_{i\in\{1,2\}} \left(f_i^{\mathrm{nw}} \mathbf{V}_i^T - \eta_i(s_i(\pi_i)) \Lambda \nabla \pi_i \right) \cdot \mathbf{n}_i^\Gamma &= 0 \quad \text{on } \Gamma \times (0, t_f), \\ \sum_{i\in\{1,2\}} \mathbf{V}_i^T \cdot \mathbf{n}_i^\Gamma &= 0 \quad \text{on } \Gamma \times (0, t_f), \end{aligned} \tag{2.13}$$

holds, where $\mathbf{n}_i^\Gamma$ denotes the unit normal vector to Γ pointing outward of Ω_i.

The following assumptions are made on the constitutive laws and physical data.

($\mathbf{A}_0$) The initial capillary pressure π_i^0 is in $L^2(\Omega_i)$.

($\mathbf{A}_1$) The porosity satisfies $0 < \underline{\phi} \le \phi(\mathbf{x}) \le \overline{\phi}$ for all $\mathbf{x} \in \Omega$ and strictly positive constants $\underline{\phi}, \overline{\phi}$.

($\mathbf{A}_2$) The saturation s_i is a strictly increasing Lipschitz continuous function from $[\underline{\pi}_i, \overline{\pi}_i]$ into $[0,1]$. Let us set $\pi^\star = \min_{i\in\{1,2\}}(\underline{\pi}_i)$ and $\pi^{\star\star} = \max_{i\in\{1,2\}}(\overline{\pi}_i)$. We assume that $s_i(\pi) = 0$ on $[\pi^\star, \underline{\pi}_i]$ and that $s_i(\pi) = 1$ on $[\underline{\pi}_i, \pi^{\star\star}]$. The saturation is extended into a strictly monotone function outside the interval $[\pi^\star, \pi^{\star\star}]$ by setting

$$s_i(u) = \begin{cases} u - \pi^\star & \text{if } u \in (-\infty, \pi^\star) \\ u - \pi^{\star\star} + 1 & \text{if } u \in (\pi^{\star\star}, +\infty) \end{cases}. \tag{2.14}$$

($\mathbf{A}_3$) The mobility M_i^{nw} (resp. M_i^{w}) is a strictly increasing (resp. strictly decreasing) Lipschitz continuous function that vanishes at 0 (resp. at 1). We extend M_i^{nw} and M_i^{w} by 0 on $(-\infty, 0)$ and $(1, +\infty)$ respectively. Hence, the fractional flow function f_i^α has the same properties. Moreover, the nonlinear diffusion function $\eta_i \ge 0$ verifies $\eta_i(0) = \eta_i(1) = 0$.

($\mathbf{A}_4$) The scalar permeability function $\Lambda \in L^\infty(\Omega)$ is such that there exist $0 < \underline{\Lambda} \le \overline{\Lambda}$ with

$$\underline{\Lambda} \le \Lambda(\mathbf{x}) \le \overline{\Lambda}, \quad \text{for a.e } \mathbf{x} \in \Omega.$$

Thanks to Assumptions ($\mathbf{A}_2$) and ($\mathbf{A}_3$), the second Kirchhoff transform ξ_i is strictly increasing and continuous on $[\underline{\pi}_i, \overline{\pi}_i]$. The inverse of ξ_i is well-defined and continuous on this interval. For technical reasons, we require a reasonable regularity on this inverse.

($\mathbf{A}_5$) The inverse of ξ_i is a Θ-Hölder function on $[\underline{\pi}_i, \overline{\pi}_i]$, for some $\Theta \in (0,1)$. This property and the Lipschitz continuity of s_i yield

$$|s_i(a) - s_i(b)| \le L_c \left|\xi_i(a) - \xi_i(b)\right|^\Theta, \quad \text{for all } a, b \in [\pi^\star, \pi^{\star\star}]. \tag{2.15}$$

Weak solution

We can finally state the definition of a weak solution to the two-phase Darcy flow model. It will be used to prove the convergence of the numerical scheme described in the next subsection.

Definition 2.1. *(Weak solution) A weak solution to the continuous model (2.5)-(2.8), (2.11)-(2.13) is a family of measurable functions $(\pi_i, P_i)_{i\in\{1,2\}}$ satisfying the following properties, for all $i \in \{1,2\}$:*

(i) $\xi_i(\pi_i), P_i \in L^2(0, t_f; H^1(\Omega_i))$,

(ii) there exists a measurable function π_Γ on $\Gamma \times (0, t_f)$ such that, for a.e. $(\boldsymbol{x}, t) \in \Gamma \times (0, t_f)$:

$$F_i(\pi_\Gamma) = \gamma_i F_i(\pi_i), \tag{2.16}$$
$$\gamma_1 P_1 - G_1^{\mathrm{nw}}(\pi_\Gamma) = \gamma_2 P_2 - G_2^{\mathrm{nw}}(\pi_\Gamma), \tag{2.17}$$

(iii) for all $\varphi, \psi \in \mathcal{C}_c^\infty(\overline{\Omega} \times [0, t_f))$, one has

$$\sum_{i\in\{1,2\}} \left(\int_{Q_{t_f}^i} \phi s_i(\pi_i) \partial_t \varphi \,\mathrm{d}\boldsymbol{x}\mathrm{d}t + \int_{\Omega_i} s_i(\pi_i^0) \varphi(\cdot, 0) \,\mathrm{d}\boldsymbol{x} \right. \\ \left. + \int_{Q_{t_f}^i} \left(f_i^{\mathrm{nw}}(s_i(\pi_i)) \mathbf{V}_i^T - \Lambda \nabla F_i(\pi_i) \right) \cdot \nabla \varphi \,\mathrm{d}\boldsymbol{x}\mathrm{d}t \right) = 0, \tag{2.18}$$

and

$$\sum_{i\in\{1,2\}} \int_{Q_{t_f}^i} \mathbf{V}_i^T \cdot \nabla \psi \,\mathrm{d}\boldsymbol{x}\mathrm{d}t = 0, \tag{2.19}$$

where the total velocity $\mathbf{V}_i^T$ is given by

$$\mathbf{V}_i^T = -M_i^T(s_i(\pi_i)) \Lambda \nabla P_i.$$

3 TPFA discretization

This section introduces our fully implicit finite volume discretization based on the total velocity formulation (2.5), on phase pressures and on capillary pressure primary unknowns. The scheme incorporates interface phase pressures and capillary pressure unknowns at all interior faces of the mesh. The discretization of the fluxes is based on a Two-Point Flux Approximation (TPFA) assuming that the mesh satisfies the orthogonality property. It results from the TPFA discretization that the face unknowns can be locally eliminated either at the linear level by a Schur complement or at the nonlinear level using a local solver for each face interface.

3.1 Space and time discretization

A spatial discretization $\mathcal{T}$ is a partition of Ω into cells consisting of convex non-overlapping open cells. Any cell $K \in \mathcal{T}$ is characterized by a point $\mathbf{x}_K \in K \setminus \partial K$ referred to as its "center". The d-Lebesgue measure of $K \in \mathcal{T}$ is denoted by $|K|$. We denote by $\mathcal{F}_K$ the set of interior faces of K, included in hyperplanes of $\mathbb{R}^d$, with $\partial K = (\partial K \cap \partial\Omega) \bigcup \left(\bigcup_{\sigma\in\mathcal{F}_K} \overline{\sigma}\right)$. For $\sigma \in \mathcal{F}_K$, we denote by $|\sigma|$ the $(d-1)$-Lebesgue measure of σ and by $\mathbf{x}_\sigma \in \sigma \setminus \partial\sigma$ the face "center" of the face σ. The orthogonality property assumes that $\mathbf{x}_\sigma$ matches with the orthogonal projection of $\mathbf{x}_K$ on σ for all $K \in \mathcal{T}$ and $\sigma \in \mathcal{F}_K$, which is assumed in the following. Let $\mathcal{F} = \bigcup_{K\in\mathcal{T}} \mathcal{F}_K$ be the set of interior faces of the mesh. It is assumed that the mesh is conforming to the interface Γ in the sense that there exists $\mathcal{F}_\Gamma \subset \mathcal{F}$ with

$$\overline{\Gamma} = \bigcup_{\sigma\in\mathcal{F}_\Gamma} \overline{\sigma}.$$

Let us also denote by $\mathcal{F}_i \subset \mathcal{F}$ the subset of faces interior to the domain $\Omega_i, i \in \{1, 2\}$, such that

$$\mathcal{F} = \mathcal{F}_1 \cup \mathcal{F}_2 \cup \mathcal{F}_\Gamma.$$

Similarly, $\mathcal{T}_i$ denotes the subset of cells of $\mathcal{T}$ included in $\overline{\Omega}_i$ with $\mathcal{T} = \mathcal{T}_1 \cup \mathcal{T}_2$. In the following the notation $\sigma = K|L$ indicates that the interior face $\sigma \in \mathcal{F}$ is shared by the two cells K and L and we set $\mathcal{T}_\sigma = \{K, L\}$. We denote by $d_{K,\sigma}$ the distance between the centers of $K \in \mathcal{T}$ and $\sigma \in \mathcal{F}_K$. The size of the mesh is defined by

$$h_\mathcal{T} = \max_{K\in\mathcal{T}} \mathrm{diam}(K).$$

Defining $\Lambda_K = \dfrac{1}{|K|}\displaystyle\int_K \Lambda(\mathbf{x})\,\mathrm{d}\mathbf{x}$ the average permeability in the cell K, the half transmissibilities and their harmonic average across a face $\sigma = K|L \in \mathcal{F}$ are given by

$$\mathbb{T}_{K,\sigma} = \frac{|\sigma|}{d_{K,\sigma}}\Lambda_K,\ K \in \mathcal{T}_\sigma, \quad \mathbb{T}_{K,L} = \frac{1}{\frac{1}{\mathbb{T}_{K,\sigma}} + \frac{1}{\mathbb{T}_{L,\sigma}}}. \tag{3.1}$$

The regularity of the mesh is characterized by the parameter $\zeta_\mathcal{T}$ such that

$$\zeta_\mathcal{T} = \min_{K\in\mathcal{T},\sigma\in\mathcal{F}_K} \frac{d_{K,\sigma}}{\mathrm{diam}(K)}. \tag{3.2}$$

For a family of finite volume meshes $(\mathcal{T}_m)_{m\in\mathbb{N}}$, it will be assumed that there exists $\zeta_0 > 0$ such that

$$\zeta_{\mathcal{T}_m} \geq \zeta_0, \qquad \text{for all } m \in \mathbb{N}.$$

For simplicity, the time discretization is assumed to be a uniform decomposition of the time interval $[0, t_f]$ into $N \in \mathbb{N}^*$ sub-intervals of size $\triangle t = t_f/N$. Let us set $t^n = n\triangle t$, for all $n \in [\![0, N]\!] := [0, N] \cap \mathbb{N}$. The extension of the discretization and of the convergence analysis to variable time stepping is straightforward.

3.2 Fully-implicit finite volume scheme

The finite volume discretization is based on the cell centered $\left(\pi_K^n, p_K^{\mathrm{nw},n}\right)_{K\in\mathcal{T}}$ and face centered $\left(\pi_\sigma^n, p_\sigma^{\mathrm{nw},n}\right)_{\sigma\in\mathcal{F}}$ primary unknowns at each time step n. The wetting phase pressures are defined by

$$p_\nu^{\mathrm{w},n} = p_\nu^{\mathrm{nw},n} - \pi_\nu^n \quad \text{for all} \quad \nu \in \mathcal{T}\cup\mathcal{F}.$$

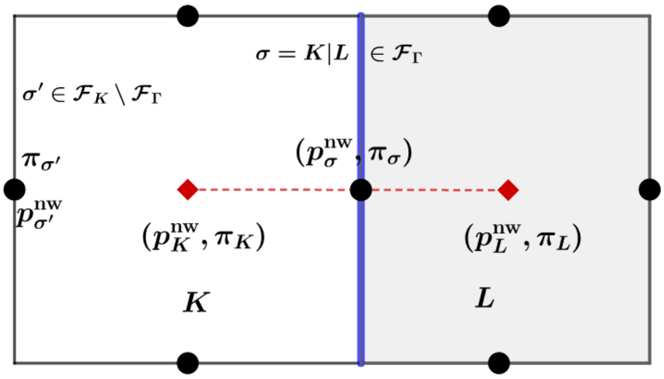

Figure 2: Example of two Cartesian cells K and L sharing the interface face $\sigma = K|L \in \mathcal{F}_\Gamma$ in bold blue. The non-wetting phase and capillary pressure primary unknowns are exhibited in both cells K and L and at the faces σ' and σ.

For all $K \in \mathcal{T}$, let us define the cell rock type $\mathrm{rt}_K = i$ for $K \subset \mathcal{T}_i$ as well as the cell porosity and initial capillary pressure as follows

$$\phi_K = \frac{1}{|K|}\int_K \phi(\mathbf{x})d\mathbf{x}, \qquad \pi_K^0 = \frac{1}{|K|}\int_K \pi^0(\mathbf{x})\,\mathrm{d}\mathbf{x}.$$

Given the approximation detailed below of the non-wetting phase flux $V_{K,\sigma}^{\mathrm{nw},n}$ and of the total flux $V_{K,\sigma}^{T,n}$ for all $\sigma\in\mathcal{F}$, $K\in\mathcal{T}_\sigma$, the finite volume discretization accounts for the volume conservation in each cell and the flux continuity equations at each interior face combined with the non-wetting phase pressure zero mean value constraint. This reads

$$\phi_K\frac{|K|}{\triangle t}\left(s_{\mathrm{rt}_K}(\pi_K^n) - s_{\mathrm{rt}_K}(\pi_K^{n-1})\right) + \sum_{\sigma\in\mathcal{F}_K} V_{K,\sigma}^{\mathrm{nw},n} = 0, \qquad \text{for all } K\in\mathcal{T}, \tag{3.3}$$

$$\sum_{\sigma\in\mathcal{F}_K} V_{K,\sigma}^{T,n} = 0, \qquad \text{for all } K\in\mathcal{T}, \tag{3.4}$$

$$V_{K,\sigma}^{\mathrm{nw},n} + V_{L,\sigma}^{\mathrm{nw},n} = 0, \qquad \text{for all } \sigma = K|L\in\mathcal{F}, \tag{3.5}$$

$$V_{K,\sigma}^{T,n} + V_{L,\sigma}^{T,n} = 0, \qquad \text{for all } \sigma = K|L\in\mathcal{F}, \tag{3.6}$$

$$\sum_{K\in\mathcal{T}} |K|\, p_K^{\mathrm{nw},n} = 0. \tag{3.7}$$

Note that all faces are treated in the same way in this approach including faces $\sigma = K|L$ with homogeneous rock types $\mathrm{rt}_K = \mathrm{rt}_L$ and faces $\sigma = K|L \in \mathcal{F}_\Gamma$ with heterogeneous rock types $\mathrm{rt}_K \neq \mathrm{rt}_L$. An alternative approach is discussed in Subsection 3.3.

The total flux approximation is defined by

$$V_{K,\sigma}^{T,n} = \mathbb{T}_{K,\sigma}\Big(M_{K,\sigma}^{\mathrm{nw},n}(p_K^{\mathrm{nw},n} - p_\sigma^{\mathrm{nw},n}) + M_{K,\sigma}^{\mathrm{w},n}(p_K^{\mathrm{w},n} - p_\sigma^{\mathrm{w},n})\Big). \tag{3.8}$$

It is based on the centered approximation of the phase mobility

$$M_{K,\sigma}^{\alpha,n} = M_{\mathrm{rt}_K}^{\alpha}(c_{K,\sigma}^n), \quad \alpha\in\{\mathrm{w},\mathrm{nw}\}, \tag{3.9}$$

designed to ensure the control of the discrete global pressure and playing a major role in the stability of the scheme, as analyzed in Subsection 3.4. The mean saturation $c^n_{K,\sigma}$ is the solution of the local nonlinear equation

$$\Big(G^{\rm w}_{{\rm rt}_K}(\pi^n_K) - G^{\rm w}_{{\rm rt}_K}(\pi^n_\sigma)\Big) M^{\rm nw}_{{\rm rt}_K}(c^n_{K,\sigma}) = \Big(G^{\rm nw}_{{\rm rt}_K}(\pi^n_K) - G^{\rm nw}_{{\rm rt}_K}(\pi^n_\sigma)\Big) M^{\rm w}_{{\rm rt}_K}(c^n_{K,\sigma}). \tag{3.10}$$

Note that, from Remark 3.1, $c^n_{K,\sigma}$ is between $s_{{\rm rt}_K}(\pi^n_K)$ and $s_{{\rm rt}_K}(\pi^n_\sigma)$.

The non-wetting phase flux approximation is defined by

$$V^{{\rm nw},n}_{K,\sigma} = f^{\rm nw}_{{\rm rt}_K}(s^{{\rm up},n}_{K,\sigma}) V^{T,n}_{K,\sigma} + \mathbb{T}_{K,\sigma}\eta^n_{K,\sigma}\Big(\pi^n_K - \pi^n_\sigma\Big), \tag{3.11}$$

combining the upwind approximation of the saturation in the fractional flow

$$s^{{\rm up},n}_{K,\sigma} = \begin{cases} s_{{\rm rt}_K}(\pi^n_K) & \text{if } V^T_{K,\sigma} \geq 0 \\ s_{{\rm rt}_K}(\pi^n_\sigma) & \text{if } V^T_{K,\sigma} < 0 \end{cases}, \tag{3.12}$$

with the approximation

$$\eta^n_{K,\sigma} = \frac{\widehat{M}^{\rm nw}_{K,\sigma}\widehat{M}^{\rm w}_{K,\sigma}}{M^T_{{\rm rt}_K}\big(s_{{\rm rt}_K}(\pi^n_K)\big)}, \tag{3.13}$$

designed to enforce the monotonicity of the capillary diffusion term, using

$$\widehat{M}^\alpha_{K,\sigma} = \max\Big\{M^\alpha_{{\rm rt}_K}\big(s_{{\rm rt}_K}(\pi^n_K)\big), M^\alpha_{{\rm rt}_K}\big(s_{{\rm rt}_K}(\pi^n_\sigma)\big)\Big\}. \tag{3.14}$$

Remark 3.1. *Note that* (3.10) *equivalently states that*

$$G^{\rm nw}_{{\rm rt}_K}(\pi^n_K) - G^{\rm nw}_{{\rm rt}_K}(\pi^n_\sigma) = (\pi^n_K - \pi^n_\sigma) f^{\rm nw}_{{\rm rt}_K}(c^n_{K,\sigma}),$$

from which we deduce that there exists π strictly between π^n_K and π^n_σ such that $c^n_{K,\sigma} = s_{{\rm rt}_K}(\pi)$. Since $f^{\rm nw}_{{\rm rt}_K}(s)$ is strictly increasing in $(0,1)$ and equal to 0 for $s \leq 0$ and to 1 for $s \geq 1$, it implies that $c^n_{K,\sigma}$ is uniquely determined in $(0,1)$. It follows that $c^n_{K,\sigma}$ depends continuously on π^n_K and π^n_σ.

Remark 3.2. *The discrete equivalent of the transmission conditions* (2.11)-(2.12)-(2.13) *at an interface $\sigma = K|L \in \mathcal{F}_\Gamma$ is obtained by the flux continuity equations* (3.5)-(3.6)*, the single value of the phase pressures $p^\alpha_\sigma = p^\alpha_{K,\sigma} = p^\alpha_{L,\sigma}$ and the two sided saturations $s_{{\rm rt}_K}(\pi_\sigma)$, $s_{{\rm rt}_L}(\pi_\sigma)$.*

3.3 Two variants of the finite volume scheme

For a given face $\sigma = K|L \in \mathcal{F}$, and given $p^{{\rm nw},n}_K, \pi^n_K, p^{{\rm nw},n}_L, \pi^n_L$, the equation (3.6) enables the computation of the interface non-wetting phase pressure $p^{{\rm nw},n}_\sigma$ in terms of the interface capillary pressure π^n_σ. Substituting the expression of $p^{{\rm nw},n}_\sigma$ in (3.5) provides the equation for π^n_σ. In practice, this equation degenerates for $\pi^n_K = \pi^n_L = \pi^\star$ (resp. for $\pi^n_K = \pi^n_L = \pi^{\star\star}$) which can be accounted for by replacing the non-wetting phase flux continuity equation by $\pi^n_\sigma = \pi^\star$ (resp. $\pi^n_\sigma = \pi^{\star\star}$). This may however yield numerical difficulties in the computation of π^n_σ. An alternative way to cope with this degeneracy is to regularize the equation (3.5) by adding an additional accumulation term as follows

$$\sum_{K\in\mathcal{T}_\sigma}\Big(\frac{\varepsilon}{\Delta t}\phi_K\,|K|\Big(s_{{\rm rt}_K}(\pi^n_\sigma) - s_{{\rm rt}_K}(\pi^{n-1}_\sigma)\Big) - V^{{\rm nw},n}_{K,\sigma}\Big) = 0, \tag{3.15}$$

where the parameter $\varepsilon > 0$ has to be chosen sufficiently small to induce a negligible perturbation of the solution. Both strategies are adopted and compared in terms of nonlinear solver efficiency in the numerical section.

Another variant of the discretization is to use face unknowns only at interfaces $\sigma \in \mathcal{F}_\Gamma$ between different rock types. Then, the flux continuity equations (3.5)-(3.6) are written only for $\sigma \in \mathcal{F}_\Gamma$. For faces $\sigma = K|L \in \mathcal{F} \setminus \mathcal{F}_\Gamma$ with $\mathrm{rt}_K = \mathrm{rt}_L$, the total flux is replaced by and expression purely based on cell unknowns:

$$V_{K,\sigma}^{T,n} = \mathbb{T}_{K,L}\Big(M_{K,L}^{\mathrm{nw},n}(p_K^{\mathrm{nw},n} - p_L^{\mathrm{nw},n}) + M_{K,L}^{\mathrm{w},n}(p_K^{\mathrm{w},n} - p_L^{\mathrm{w},n})\Big), \tag{3.16}$$

with

$$M_{K,L}^{\alpha,n} = M_{\mathrm{rt}_K}^{\alpha}(c_{K,L}^n), \quad \alpha \in \{\mathrm{w}, \mathrm{nw}\}, \tag{3.17}$$

where $c_{K,L}^n$ is the solution of the local nonlinear equation

$$\Big(G_{\mathrm{rt}_K}^{\mathrm{w}}(\pi_K^n) - G_{\mathrm{rt}_K}^{\mathrm{w}}(\pi_L^n)\Big)M_{\mathrm{rt}_K}^{\mathrm{nw}}(c_{K,L}^n) = \Big(G_{\mathrm{rt}_K}^{\mathrm{nw}}(\pi_K^n) - G_{\mathrm{rt}_K}^{\mathrm{nw}}(\pi_L^n)\Big)M_{\mathrm{rt}_K}^{\mathrm{w}}(c_{K,L}^n). \tag{3.18}$$

Similarly, the non-wetting phase flux is modified as

$$V_{K,\sigma}^{\mathrm{nw},n} = f_{\mathrm{rt}_K}^{\mathrm{nw}}(s_{K,L}^{\mathrm{up},n})V_{K,\sigma}^{T,n} + \mathbb{T}_{K,L}\eta_{K,L}^n\Big(\pi_K^n - \pi_L^n\Big), \tag{3.19}$$

with

$$s_{K,L}^{\mathrm{up},n} = \begin{cases} s_{\mathrm{rt}_K}(\pi_K^n) & \text{if } V_{K,\sigma}^T \geq 0 \\ s_{\mathrm{rt}_K}(\pi_L^n) & \text{if } V_{K,\sigma}^T < 0 \end{cases}, \tag{3.20}$$

and

$$\eta_{K,L}^n = \frac{\widehat{M}_{K,L}^{\mathrm{nw}}\widehat{M}_{K,L}^{\mathrm{w}}}{\mathbb{T}_{K,L}\Big(\frac{M_{\mathrm{rt}_K}^T(s_{\mathrm{rt}_K}(\pi_K^n))}{\mathbb{T}_{K,\sigma}} + \frac{M_{\mathrm{rt}_K}^T(s_{\mathrm{rt}_K}(\pi_L^n))}{\mathbb{T}_{L,\sigma}}\Big)}, \tag{3.21}$$

using

$$\widehat{M}_{K,L}^{\alpha} = \max\Big\{M_{\mathrm{rt}_K}^{\alpha}\big(s_{\mathrm{rt}_K}(\pi_K^n)\big), M_{\mathrm{rt}_K}^{\alpha}\big(s_{\mathrm{rt}_K}(\pi_L^n)\big)\Big\}. \tag{3.22}$$

In the numerical section, this variant will be compared in terms of accuracy to the scheme of Subsection 3.2 with unknowns at all faces $\sigma \in \mathcal{F}$.

Note that the following stability and convergence analysis is only carried out for the original scheme of Subsection 3.2 but it can be extended to both variants of the scheme.

3.4 Stability estimates and existence result

Let us first prove the existence of a solution to the local interface system.

Lemma 3.3. *For each $\sigma = K|L \in \mathcal{F}$ and for any $(p_K^{\mathrm{nw},n}, p_L^{\mathrm{nw},n}, \pi_K^n, \pi_L^n) \in \mathbb{R}^4$, there exists $(p_\sigma^{\mathrm{nw},n}, \pi_\sigma^n)$, with $\pi_\sigma^n \in [\pi^\star, \pi^{\star\star}]$, solving the local nonlinear system*

$$\begin{cases} V_{K,\sigma}^{\mathrm{nw},n} + V_{L,\sigma}^{\mathrm{nw},n} &= 0, \\ V_{K,\sigma}^{T,n} + V_{L,\sigma}^{T,n} &= 0. \end{cases} \tag{3.23}$$

Proof. The superscript n is omitted in the following. From remarks 3.1, solving the equation $V_{K,\sigma}^T + V_{L,\sigma}^T = 0$ w.r.t. p_σ^{nw}, we can express $V_{K,\sigma}^T = -V_{L,\sigma}^T$ as a continuous function of π_σ. Next, let us define

$$\Psi(\pi_\sigma) = V_{K,\sigma}^{\mathrm{nw}}(\pi_\sigma) + V_{L,\sigma}^{\mathrm{nw}}(\pi_\sigma),$$

as a function of π_σ considering the total velocities $V_{K,\sigma}^T$ and $V_{L,\sigma}^T$ as functions of π_σ. One can show from the definition of the fluxes $V_{K,\sigma}^{\mathrm{nw}}$, $V_{L,\sigma}^{\mathrm{nw}}$ that $\Psi(\pi^\star) \geq 0$ and $\Psi(\pi^{\star\star}) \leq 0$. Then, we deduce from the continuity of the function $\Psi(\pi_\sigma)$ the existence of a solution $\pi_\sigma \in [\pi^\star, \pi^{\star\star}]$ to the equation $\Psi(\pi_\sigma) = 0$. By construction, one also infers the existence of p_σ^{nw}, which concludes the proof. □

Remark 3.4. *Note that for faces $\sigma = K|L \in \mathcal{F} \setminus \mathcal{F}_\Gamma$ with $\mathrm{rt}_K = \mathrm{rt}_L$, it is easy to adapt the previous proof to show that there exists a solution $(p_\sigma^{\mathrm{nw},n}, \pi_\sigma^n)$ to (3.23) such that $\pi_\sigma^n \in [\underline{\pi}_{\mathrm{rt}_K}, \overline{\pi}_{\mathrm{rt}_K}]$.*

Next, we need to ensure that the computed capillary pressure remains in its initial range.

Lemma 3.5. *Let us assume that $\pi^\star \le \pi_K^0 \le \pi^{\star\star}$, for all $K \in \mathcal{T}$ and that the solution of the local interface system (3.23) is chosen according to Lemma 3.3 such that $\pi_\sigma^n \in [\pi^\star, \pi^{\star\star}]$ for all $\sigma \in \mathcal{F}$ and $n \in [\![0, N]\!]$. Then, any solution of (3.3)-(3.4)is such that the discrete capillary pressure satisfies the following L^∞ bound*

$$\pi^\star \le \pi_K^n \le \pi^{\star\star}, \quad \forall K \in \mathcal{T},\ \forall n \in [\![1, N]\!]. \tag{3.24}$$

Proof. The result is shown by induction on n. The property is trivial for $n = 0$. We only detail the inductive step for the lower bound

$$\pi_K^n \ge \pi^\star, \qquad \forall K \in \mathcal{T},\ \forall n \in [\![1, N]\!],$$

the case of the upper bound being similar. We first set K a cell such that $\pi_K^n = \min_{L\in\mathcal{T}} \pi_L^n$. Assume that $\pi_K^n < \pi^\star$. Multiplying the saturation equation corresponding to the cell K by $\pi_K^n - \pi^\star$ gives

$$\underbrace{\phi_K \frac{|K|}{\Delta t}\Big(s_{\mathrm{rt}_K}(\pi_K^n)(\pi_K^n - \pi^\star) - s_{\mathrm{rt}_K}(\pi_K^{n-1})(\pi_K^n - \pi^\star)\Big)}_{A_K} + \sum_{\sigma\in\mathcal{F}_K} \underbrace{V_{K,\sigma}^{\mathrm{nw}}(\pi_K^n, \pi_\sigma^n)(\pi_K^n - \pi^\star)}_{B_{K,\sigma}} = 0.$$

Developping the expression of $B_{K,\sigma}$ leads to

$$\begin{aligned} B_{K,\sigma} &= f_{\mathrm{rt}_K}^{\mathrm{nw}}\left(s_{\mathrm{rt}_K}(\pi_K^n)\right)\left(V_{K,\sigma}^T\right)^+(\pi_K^n - \pi^\star) - f_{\mathrm{rt}_K}^{\mathrm{nw}}\left(s_{\mathrm{rt}_K}(\pi_\sigma^n)\right)\left(V_{K,\sigma}^T\right)^-(\pi_K^n - \pi^\star) \\ &\quad + \mathbb{T}_{K,\sigma}\eta_{K,\sigma}^n\left(\pi_K^n - \pi_\sigma^n\right)(\pi_K^n - \pi^\star). \end{aligned}$$

Bear in mind that, since $\pi_K^n < \pi^\star$, we have $s_{\mathrm{rt}_K}(\pi_K^n) = \pi_K^n - \pi^\star < 0$ and that the function $f_{\mathrm{rt}_K}^{\mathrm{nw}}$ vanishes on $(-\infty, 0]$. Hence

$$f_{\mathrm{rt}_K}^{\mathrm{nw}}\left(s_{\mathrm{rt}_K}(\pi_K^n)\right)\left(V_{K,\sigma}^T\right)^+(\pi_K^n - \pi^\star) = 0.$$

Now, since $\pi_\sigma^n - \pi^\star \ge 0$, we deduce that $B_{K,\sigma}$ is nonnegative for all $\sigma \in \mathcal{F}_K$. Consequently, $A_K \ge 0$. By induction hypothesis, $s_{\mathrm{rt}_K}(\pi_K^{n-1}) \ge 0$ and, thus, the extension of the saturation function given by Assumption $(\mathbf{A}_2)$ gives

$$s_{\mathrm{rt}_K}(\pi_K^n)(\pi_K^n - \pi^\star) = (\pi_K^n - \pi^\star)^2 \le 0.$$

This proves that $\pi_K^n = \pi^\star$, contradicting the assumption $\pi_K^n < \pi^\star$ and concluding the proof. $\square$

Remark 3.6. *It is possible to improve the bounds of the inequality (3.24) by adapting the previous proof. The computed capillary pressure π_K^n for each cell $K \in \mathcal{T}$ stays within the range $(\underline{\pi}_{\mathrm{rt}_K}, \overline{\pi}_{\mathrm{rt}_K})$ of the initial capillary pressure. To prove this, different extensions of the saturation function must be introduced in Assumption $(\boldsymbol{A}_2)$. For cells $K \in \mathcal{T}$ and homogeneous interfaces $\sigma = K|L \in \mathcal{F} \setminus \mathcal{F}_\Gamma$ the extension is done outside the range $(\underline{\pi}_{\mathrm{rt}_K}, \overline{\pi}_{\mathrm{rt}_K})$ while for heterogeneous interfaces $\sigma \in \mathcal{F}_\Gamma$, the extension is kept outside the range $(\pi^\star, \pi^{\star\star})$. This would make the notations heavier and is the reason why we restricted ourselves to the bounds $\pi^\star$ and $\pi^{\star\star}$ in all cases.*

We are next interested in establishing energy estimates. The proof of the estimations below requires the use of the global pressure. A discrete counterpart of (2.10) is defined by

$$P_K^n = p_K^{\mathrm{w},n} + G_{\mathrm{rt}_K}^{\mathrm{nw}}(\pi_K^n) = p_K^{\mathrm{nw},n} - G_{\mathrm{rt}_K}^{\mathrm{w}}(\pi_K^n),$$

where the second equality derives from $p_K^{\mathrm{nw},n} - p_K^{\mathrm{w},n} = \pi_K^n$ and $G_{\mathrm{rt}_K}^{\mathrm{nw}}(\pi_K^n) + G_{\mathrm{rt}_K}^{\mathrm{w}}(\pi_K^n) = \pi_K^n$. Similarly, the global pressure at face $\sigma = K|L \in \mathcal{F}$ reads

$$P_{K,\sigma}^n = p_\sigma^{\mathrm{w},n} + G_{\mathrm{rt}_K}^{\mathrm{nw}}(\pi_\sigma^n) = p_\sigma^{\mathrm{nw},n} - G_{\mathrm{rt}_K}^{\mathrm{w}}(\pi_\sigma^n),$$

from which we deduce the discrete equivalent of the transmission condition (2.11)

$$P_{K,\sigma}^n - G_{\mathrm{rt}_K}^{\mathrm{nw}}(\pi_\sigma^n) = P_{L,\sigma}^n - G_{\mathrm{rt}_L}^{\mathrm{nw}}(\pi_\sigma^n).$$

A key consequence of our choice of the mobilities (3.9)-(3.10) in the definition (3.8) of $V_{K,\sigma}^{T,n}$ is that the total flux rewrites

$$V_{K,\sigma}^{T,n} = M_{\mathrm{rt}_K}^T(c_{K,\sigma}^n)\mathbb{T}_{K,\sigma}\Big(P_K^n - P_{K,\sigma}^n\Big). \tag{3.25}$$

Unless mentioned, we denote by C a generic positive constant depending only on the data and possibly on the mesh regularity $\zeta_{\mathcal{T}}$ defined in (3.2), but not on the discretization parameters.

Proposition 3.7. *Let $(p_\nu^{\mathrm{nw},n}, \pi_\nu^n)_{\nu\in\mathcal{T}\cup\mathcal{F}}$, $n \in [\![1,N]\!]$ be a solution of the finite volume scheme (3.3)-(3.7), then there exists a positive constant C such that*

$$\sum_{n=1}^N \triangle t \sum_{K\in\mathcal{T}} \sum_{\sigma\in\mathcal{F}_K} \mathbb{T}_{K,\sigma}\eta_{K,\sigma}^n \Big(\pi_K^n - \pi_\sigma^n\Big)^2 \le C, \tag{3.26}$$

$$\sum_{n=1}^N \triangle t \sum_{K\in\mathcal{T}} \sum_{\sigma\in\mathcal{F}_K} \mathbb{T}_{K,\sigma}\Big(\xi_{\mathrm{rt}_K}(\pi_K^n) - \xi_{\mathrm{rt}_K}(\pi_\sigma^n)\Big)^2 \le C, \tag{3.27}$$

$$\sum_{n=1}^N \triangle t \sum_{K\in\mathcal{T}} \sum_{\sigma\in\mathcal{F}_K} \mathbb{T}_{K,\sigma}(P_K^n - P_{K,\sigma}^n)^2 \le C. \tag{3.28}$$

Proof. Let us first estimate the capillary terms. Multiplying equation (3.3) by $\triangle t\ \pi_K^n$ and equation (3.5) by $\triangle t\ \pi_\sigma^n$ and summing over $K \in \mathcal{T}$, $\sigma \in \mathcal{F}$ and $n \in [\![1,N]\!]$ gives

$$X + Y + Z = 0, \tag{3.29}$$

where

$$X = \sum_{n=1}^N \sum_{K\in\mathcal{T}} \phi_K\,|K|\,\Big(s_{\mathrm{rt}_K}(\pi_K^n) - s_{\mathrm{rt}_K}(\pi_K^{n-1})\Big)\pi_K^n,$$

$$Y = \sum_{n=1}^N \triangle t \sum_{K\in\mathcal{T}} \sum_{\sigma\in\mathcal{F}_K} f_{\mathrm{rt}_K}^{\mathrm{nw}}(s_{K,\sigma}^{\mathrm{up},n})V_{K,\sigma}^T\Big(\pi_K^n - \pi_\sigma^n\Big),$$

$$Z = \sum_{n=1}^N \triangle t \sum_{K\in\mathcal{T}} \sum_{\sigma\in\mathcal{F}_K} \mathbb{T}_{K,\sigma}\eta_{K,\sigma}^n\Big(\pi_K^n - \pi_\sigma^n\Big)^2.$$

By virtue of Assumption $(\mathbf{A}_2)$, let us recall that $s_i' \in L^\infty(\pi^\star, \pi^{\star\star})$. Let us consider $\Pi_i(v) = \displaystyle\int_0^v u s_i'(u)\,\mathrm{d}u$. Integrating by parts and recalling that s_i is increasing, we observe that

$$\Pi_i(v) - \Pi_i(w) = v\big(s_i(v) - s_i(w)\big) - \int_w^v \big(s_i(u) - s_i(w)\big)\,\mathrm{d}u \le v\big(s_i(v) - s_i(w)\big).$$

Then, a telescopic sum yields

$$X \geq \sum_{K\in\mathcal{T}} \phi_K\,|K|\,\Big(\Pi_{\mathrm{rt}_K}(\pi_K^N) - \Pi_{\mathrm{rt}_K}(\pi_K^0)\Big). \tag{3.30}$$

Using the convexity of the function $G^{\mathrm{nw}}_{\mathrm{rt}_K}$ defined in (2.9) and the upstream choice (3.12) we deduce that

$$Y \geq \sum_{n=1}^{N} \triangle t \sum_{K\in\mathcal{T}}\sum_{\sigma\in\mathcal{F}_K} V^T_{K,\sigma}\Big(G^{\mathrm{nw}}_{\mathrm{rt}_K}(\pi^n_K) - G^{\mathrm{nw}}_{\mathrm{rt}_K}(\pi^n_\sigma)\Big) =: E_1. \tag{3.31}$$

At this stage, we need to consider the energy estimation on the global pressure. Multiplying equation (3.4) by $\triangle t\ (P^n_K - G^{\mathrm{nw}}_{\mathrm{rt}_K}(\pi^n_K))$, equation (3.6) by $\triangle t\ (P^n_{K,\sigma} - G^{\mathrm{nw}}_{\mathrm{rt}_K}(\pi^n_\sigma))$, using (3.25) and summing over $K\in\mathcal{T}$, $\sigma\in\mathcal{F}$ and $n\in[\![1,N]\!]$, we obtain

$$E_1 = \sum_{n=1}^{N} \triangle t \sum_{K\in\mathcal{T}}\sum_{\sigma\in\mathcal{F}_K} M^T_{\mathrm{rt}_K}(c^n_{K,\sigma})\mathbb{T}_{K,\sigma}(P^n_K - P^n_{K,\sigma})^2. \tag{3.32}$$

Now, by the boundedness from below of the total mobility $M^T_{\mathrm{rt}_K}(s) \geq m_0$ for all $s\in(0,1)$,

$$Y \geq m_0 \sum_{n=1}^{N} \triangle t \sum_{K\in\mathcal{T}}\sum_{\sigma\in\mathcal{F}_K} \mathbb{T}_{K,\sigma}(P^n_K - P^n_{K,\sigma})^2. \tag{3.33}$$

As a consequence of (3.29), (3.30) and (3.33) we infer

$$\begin{aligned}\sum_{n=1}^{N} \triangle t \sum_{K\in\mathcal{T}}\sum_{\sigma\in\mathcal{F}_K} \mathbb{T}_{K,\sigma}\eta^n_{K,\sigma}\Big(\pi^n_K - \pi^n_\sigma\Big)^2&\\ + m_0 \sum_{n=1}^{N} \triangle t \sum_{K\in\mathcal{T}}\sum_{\sigma\in\mathcal{F}_K} \mathbb{T}_{K,\sigma}(P^n_K - P^n_{K,\sigma})^2 \leq C,&\end{aligned} \tag{3.34}$$

for some constant $C>0$ depending only on π_0 and $\overline{\phi}$. This implies (3.26) and (3.28). Finally, observe that

$$\sqrt{\eta^n_{K,\sigma}} \geq \max_{a\in I^n_{K,\sigma}} \xi'_{\mathrm{rt}_K}(a),$$

where $I^n_{K,\sigma} = [\min(\pi^n_K,\pi^n_\sigma), \max(\pi^n_K,\pi^n_\sigma)]$. Thanks to this inequality and to (3.34), the inequality (3.27) holds true. The proof is concluded. $\square$

Proposition 3.8. *The fully implicit finite volume scheme* (3.3)-(3.7) *has a solution* $(p^{\mathrm{nw},n}_\nu, \pi^n_\nu)_{\nu\in\mathcal{T}\cup\mathcal{F}}$ *at each time iteration* $n\in[\![1,N]\!]$*, such that* $\pi^n_\nu\in[\pi^\star,\pi^{\star\star}]$ *for all* $\nu\in\mathcal{T}\cup\mathcal{F}$*.*

Proof. The proof of the existence result uses a topological degree technique [16]. To this end, we perturb some physical laws by introducing the parameter $\lambda\in[0,1]$ as follows

$$\begin{aligned}&M^{\mathrm{nw},\lambda}_i(s^{\mathrm{nw}}) = \lambda M^{\mathrm{nw}}_i(s^{\mathrm{nw}}) + (1-\lambda)s^{\mathrm{nw}},\\ &M^{\mathrm{w},\lambda}_i(s^{\mathrm{nw}}) = \lambda M^{\mathrm{w}}_i(s^{\mathrm{nw}}) + (1-\lambda)(1-s^{\mathrm{nw}}),\\ &\pi^\lambda_i = \lambda\pi_i + (1-\lambda)\pi_1.\end{aligned}$$

Let us denote by $V^{\mathrm{nw},\lambda}_{K,\sigma}$ the corresponding expression of the non-wetting phase velocity when considering the above physical functions depending on λ. We modify equation (3.5) by

$$V^{\mathrm{nw},\lambda}_{K,\sigma} + V^{\mathrm{nw},\lambda}_{L,\sigma} + \max(\pi^\star - \pi_\sigma, 0) + \min(\pi^{\star\star} - \pi_\sigma, 0) = 0, \tag{3.35}$$

such that one ensures that any solution of the modified interface problem is such that π_σ stays in $[\pi^\star, \pi^{\star\star}]$. We also replace the constraint (3.7) by

$$\sum_{K\in\mathcal{T}} |K| \left(\lambda p_K^{\mathrm{nw},n} + (1-\lambda) P_K^n\right) = 0.$$

Applying the same procedure as above one can prove that any solution $(p_\nu^{\mathrm{nw},\lambda,n}, \pi_\nu^{\lambda,n})_{\nu\in\mathcal{T}\cup\mathcal{F}}$ of the modified scheme is such that $\pi_\nu^{\lambda,n} \in [\pi^\star, \pi^{\star\star}]$ for all $\nu \in \mathcal{T}\cup\mathcal{F}$ and such that Proposition 3.7 still holds with a constant independent of λ. Then, for $\lambda = 0$ we get a homogeneous decoupled finite volume scheme. The remaining part of the proof is a straightforward adaption of the one given in [7, Proposition 3.6]. □

4 Convergence analysis

This section addresses the convergence of the numerical scheme. Let $(\mathcal{T}_m)_{m\in\mathbb{N}}$ be a sequence of discretizations of the domain Ω in the sense of Subsection 3.1, such that $h_{\mathcal{T}_m}$ goes to zero as m tends to $+\infty$ and such that $\inf_{m\in\mathbb{N}} \zeta_{\mathcal{T}_m} > 0$.

Let $\mathcal{T}_{i,m}$ be the subset of cells of $\mathcal{T}_m$ included in $\overline{\Omega}_i$ for $i \in \{1,2\}$. The set of interior faces is denoted by $\mathcal{F}_m$, its subset of interior faces of Ω_i by $\mathcal{F}_{i,m}$, and its subset of interface faces by $\mathcal{F}_{\Gamma,m}$. Let us also consider a sequence of uniform time discretization $\triangle t_m$ of the time interval $(0, t_f)$ with N_m time steps such that $\triangle t_m$ tends to zero as m goes to $+\infty$.

Let us introduce the vector space $X_{i,m}$ defined by

$$X_{i,m} = \left\{ u_{\mathcal{D}_{i,m}} = \left((u_K)_{K\in\mathcal{T}_{i,m}}, (u_\sigma)_{\sigma\in\mathcal{F}_{i,m}}, (u_{i,\sigma})_{\sigma\in\mathcal{F}_{\Gamma,m}}\right);\ u_K \in \mathbb{R},\ u_\sigma \in \mathbb{R},\ u_{i,\sigma} \in \mathbb{R} \right\}, \quad (4.1)$$

and its subspace $X_{i,m}^0$ of vectors $u_{\mathcal{D}_{i,m}} \in X_{i,m}$ such that $u_{i,\sigma} = 0$ for $\sigma \in \mathcal{F}_{\Gamma,m}$.

Let $(u_{\mathcal{D}_{1,m}}, u_{\mathcal{D}_{2,m}}) \in X_{1,m} \times X_{2,m}$, note that the components of $u_{\mathcal{D}_{1,m}}$ and $u_{\mathcal{D}_{2,m}}$ on both sides of the interface for $\sigma \in \mathcal{F}_{\Gamma,m}$, either have the same values $u_{1,\sigma} = u_{2,\sigma} = u_\sigma$, as it is the case for

$$\pi^n_{\mathcal{D}_{i,m}} = \left((\pi_K^n)_{K\in\mathcal{T}_{i,m}}, (\pi_\sigma^n)_{\sigma\in\mathcal{F}_{i,m}\cup\mathcal{F}_{\Gamma,m}}\right) \text{ and } p^{\alpha,n}_{\mathcal{D}_{i,m}} = \left((p_K^{\alpha,n})_{K\in\mathcal{T}_{i,m}}, (p_\sigma^{\alpha,n})_{\sigma\in\mathcal{F}_{i,m}\cup\mathcal{F}_{\Gamma,m}}\right),$$

or different values like for

$$P^n_{\mathcal{D}_{i,m}} = \left((P_K^n)_{K\in\mathcal{T}_{i,m}}, (P_{K,\sigma}^n = P_{L,\sigma}^n)_{\sigma=K|L\in\mathcal{F}_{i,m}}, (P_{K,\sigma}^n)_{\sigma\in\mathcal{F}_{\Gamma,m},\{K\}=\mathcal{T}_\sigma\cap\mathcal{T}_{i,m}}\right),$$

$$s^n_{\mathcal{D}_{i,m}} = \left((s_i(\pi_K^n))_{K\in\mathcal{T}_{i,m}}, (s_i(\pi_\sigma^n))_{\sigma\in\mathcal{F}_{i,m}}, (s_i(\pi_\sigma^n))_{\sigma\in\mathcal{F}_{\Gamma,m}}\right).$$

Similarly, $F^n_{\mathcal{D}_{i,m}}$ (resp. $\xi^n_{\mathcal{D}_{i,m}}$) is defined with the function F_i (resp. ξ_i) as for s_i. Note that for $u_{\mathcal{D}_{i,m}} \in X_{i,m}$ and any $\sigma \in \mathcal{F}_{\Gamma,m}$, we will also denote $u_{i,\sigma}$ by $u_{K,\sigma}$ for $\{K\} = \mathcal{T}_\sigma \cap \mathcal{T}_{i,m}$ if we have two different values at both sides of the interface or simply by u_σ if only a single value is available. Likewise, for $\sigma = K|L \in \mathcal{F}_{i,m}$ we will make use of the notations $u_\sigma = u_{K,\sigma} = u_{L,\sigma}$.

The space $X_{i,m}$ is equipped with the semi-norm

$$\|u_{\mathcal{D}_{i,m}}\|_{1,\mathcal{D}_{i,m}} = \left(\sum_{K\in\mathcal{T}_{i,m}} \sum_{\sigma\in\mathcal{F}_K} \mathbb{T}_{K,\sigma}(u_K - u_{K,\sigma})^2\right)^{1/2}. \quad (4.2)$$

For any $u_{\mathcal{D}_{i,m}} \in X_{i,m}$ let us define the cellwise constant function reconstruction operator by

$$\Pi_{\mathcal{T}_{i,m}} u_{\mathcal{D}_{i,m}} := \sum_{K\in\mathcal{T}_{i,m}} u_K \mathbf{1}_K,$$

where $\mathbf{1}_K$ is the characteristic function of K. Note that $\Pi_{\mathcal{T}_{i,m}} u_{\mathcal{D}_{i,m}}$ is defined on $\mathbb{R}^d$ and vanishes outside Ω_i. For convenience, we will use in the following the shorter notation

$$u_{\mathcal{T}_{i,m}} = \Pi_{\mathcal{T}_{i,m}} u_{\mathcal{D}_{i,m}}.$$

Let $Y_{i,m} = \Pi_{\mathcal{T}_{i,m}} X_{i,m}$. We denote by $\mathcal{Y}_{i,m}$ the vector space $Y_{i,m}$ equipped with the norm

$$\left\| v_{\mathcal{T}_{i,m}} \right\|_{\mathcal{Y}_{i,m}} = \left\| v_{\mathcal{T}_{i,m}} \right\|_{L^1(\Omega_i)} + \sup_{\mathbf{y}\in\mathbb{R}^d, \mathbf{y}\neq 0} \frac{\left\| v_{\mathcal{T}_{i,m}}(\cdot + \mathbf{y}) - v_{\mathcal{T}_{i,m}} \right\|_{L^1(\Omega_i)}}{|\mathbf{y}|^{\Theta}},$$

and by $\mathbb{Y}_{i,m}$ the vector space $Y_{i,m}$ equipped with the dual norm

$$\left\| v_{\mathcal{T}_{i,m}} \right\|_{\mathbb{Y}_{i,m}} = \sup \left\{ \int_{\Omega_i} \phi_i(\mathbf{x}) v_{\mathcal{T}_{i,m}}(\mathbf{x}) \psi_{\mathcal{T}_{i,m}}(\mathbf{x})\,\mathrm{d}\mathbf{x} \ : \ \psi_{\mathcal{D}_{i,m}} \in X^0_{i,m},\ \left\| \psi_{\mathcal{D}_{i,m}} \right\|_{1,\mathcal{D}_{i,m}} \leq 1 \right\}.$$

For any $u_{\mathcal{D}_{i,m}} \in X_{i,m}$, let us define the two-point gradient reconstruction operator by

$$\nabla_{\mathcal{D}_{i,m}} u_{\mathcal{D}_{i,m}} = \sum_{K\in\mathcal{T}_{i,m}} \sum_{\sigma\in\mathcal{F}_K} d \frac{u^n_{K,\sigma} - u^n_K}{d_{K,\sigma}} \mathbf{n}_{K,\sigma} \mathbf{1}_{D_{K,\sigma}},$$

where $D_{K,\sigma}$ is the pyramid with base σ and apex $\mathbf{x}_K$.

For any $u_{\mathcal{D}_{i,m}} \in X_{i,m}$, we also use the function reconstruction operator defined by

$$\Pi_{\mathcal{D}_{i,m}} u_{\mathcal{D}_{i,m}} := \sum_{K\in\mathcal{T}_{i,m}} \sum_{\sigma\in\mathcal{F}_K} u_\sigma \mathbf{1}_{D_{K,\sigma}}.$$

Let $u_{\mathcal{D}_{i,m}} = (u^1_{\mathcal{D}_{i,m}}, \cdots, u^{N_m}_{\mathcal{D}_{i,m}}) \in (X_{i,m})^{N_m}$. The previous function and gradient spatial reconstruction operators (say $\mathcal{O}_{i,m} = \Pi_{\mathcal{T}_{i,m}}, \Pi_{\mathcal{D}_{i,m}}, \nabla_{\mathcal{D}_{i,m}}$) are extended to space time reconstruction operators such that, keeping the same notation for legibility,

$$\mathcal{O}_{i,m} u_{\mathcal{D}_{i,m}}(\cdot, t) = \mathcal{O}_{i,m} u^n_{\mathcal{D}_{i,m}} \text{ for all } t \in (t^{n-1}, t^n], \quad n \in [\![1, N]\!].$$

If $g : \mathbb{R} \to \mathbb{R}$ is a continuous function and $u_{\mathcal{D}_{i,m}} \in X_{\mathcal{D}_{i,m}}$, we denote by $g(u_{\mathcal{D}_{i,m}}) \in X_{\mathcal{D}_{i,m}}$ the vector

$$g(u_{\mathcal{D}_{i,m}}) = \Big((g(u_K))_{K\in\mathcal{T}_{i,m}}, (g(u_\sigma))_{\sigma\in\mathcal{F}_{i,m}}, (g(u_{i,\sigma}))_{\sigma\in\mathcal{F}_{\Gamma,m}} \Big).$$

Note that the piecewise constant function reconstruction operators $\Pi_{\mathcal{T}_{i,m}}$ and $\Pi_{\mathcal{D}_{i,m}}$ commute with the above definition of $g(u_{\mathcal{D}_{i,m}})$, that is, for example, $\Pi_{\mathcal{T}_{i,m}} g(u_{\mathcal{D}_{i,m}}) = g(\Pi_{\mathcal{T}_{i,m}} u_{\mathcal{D}_{i,m}})$.

Let us now state the convergence theorem summing up the convergence results, that will be established in the following subsections.

Theorem 4.1. *Let $(\mathcal{T}_{i,m}, \triangle t_m)_{m\in\mathbb{N}}$ be a sequence of discretizations of $Q^i_{t_f}$ such that $h_{\mathcal{T}_{i,m}}$ and $\triangle t_m$ go to zero as m tends to $+\infty$, and $\inf_{m\in\mathbb{N}} \zeta_{\mathcal{T}_m} > 0$. Let $(\pi_{\mathcal{T}_{i,m}}, p^{\mathrm{nw}}_{\mathcal{T}_{i,m}})_{m\in\mathbb{N}}$ be the corresponding sequence of discrete solutions to the finite volume scheme (3.3)-(3.7). Then, there exist $\pi_i \in L^2(Q^i_{t_f})$ with $\xi_i(\pi_i) \in L^2(0, t_f; H^1(\Omega))$, $p^\alpha_i \in L^2(Q^i_{t_f})$, and $P_i \in L^2(0, t_f; H^1(\Omega_i))$ such that $\pi_i = p^{\mathrm{nw}}_i - p^{\mathrm{w}}_i$ and, up to a subsequence as m tends to $+\infty$,*

$$\begin{aligned}
&s_{\mathcal{T}_{i,m}} \longrightarrow s_i(\pi_i) && \text{a.e. in } Q^i_{t_f} \text{ and strongly in } L^1(Q^i_{t_f}),\\
&p^\alpha_{\mathcal{T}_{i,m}} \longrightarrow p^\alpha_i && \text{weakly } L^2(Q^i_{t_f}),\\
&\nabla_{\mathcal{D}_{i,m}} F_i(\pi_{\mathcal{D}_{i,m}}) \longrightarrow \nabla F_i(\pi_i) && \text{weakly } L^2(Q^i_{t_f})^d,\\
&\nabla_{\mathcal{D}_{i,m}} P_{\mathcal{D}_{i,m}} \longrightarrow \nabla P_i && \text{weakly } L^2(Q^i_{t_f})^d.
\end{aligned}$$

The limit functions $(\pi_i, P_i)_{i\in\{1,2\}}$ satisfy the variational formulation (2.18)-(2.19) as well as the transmission condition (2.16) and (2.17) given in Definition 2.1.

The proof of the above theorem is deduced from a combination of several results outlined as follows. First, the strong convergence of the saturation and the weak convergence of the discrete gradients are stated in Proposition 4.5. Next, in Proposition 4.6 we prove that the limits $(\pi_i, P_i)_{i\in\{1,2\}}$ satisfy the weak formulation. Finally, to show that the limits satisfy the transmission conditions, an alternative proof to the one presented in [7] is proposed in Subsection 4.3 for the convergence of the discrete traces.

4.1 Convergence of the finite volume scheme

The following proposition provides a key compactness property of the sequence $(\mathcal{Y}_{i,m}, \mathbb{Y}_{i,m})_{m\in\mathbb{N}}$.

Proposition 4.2. *The sequence $(\mathcal{Y}_{i,m}, \mathbb{Y}_{i,m})_m$ is compactly-continuously embedded in $L^1(\Omega_i)$ in the sense of [19, Definition C.6].*

Proof. Step 1. Let $(u_{\mathcal{T}_{i,m}})_{m\in\mathbb{N}}$ be a sequence such that

$$u_{\mathcal{T}_{i,m}} \in \mathcal{Y}_{i,m} \text{ for all } m \in \mathbb{N}, \text{ and } \left(\left\|u_{\mathcal{T}_{i,m}}\right\|_{\mathcal{Y}_{i,m}}\right)_{m\in\mathbb{N}} \text{ is bounded .}$$

As a consequence of the definition of the norm $\mathcal{Y}_{i,m}$, there exists $C > 0$ such that

$$\left\|u_{\mathcal{T}_{i,m}}(\cdot + \mathbf{y}) - u_{\mathcal{T}_{i,m}}\right\|_{L^1(\Omega_i)} \leq C\,|\mathbf{y}|^{\Theta}, \quad \text{for all } \mathbf{y} \in \mathbb{R}^d.$$

In light of Kolmogorov's compactness theorem, this ensures the existence of a subsequence of $(u_{\mathcal{T}_{i,m}})_{m\in\mathbb{N}}$ that converges towards u_i in $L^1(\Omega_i)$.

Step 2. Let $(v_{\mathcal{T}_{i,m}})_{m\in\mathbb{N}}$ be a sequence such that
(i) $v_{\mathcal{T}_{i,m}} \in Y_{i,m}$ for all $m \in \mathbb{N}$ and $(\left\|v_{\mathcal{T}_{i,m}}\right\|_{\mathcal{Y}_{i,m}})_{m\in\mathbb{N}}$ is bounded,
(ii) $\left\|v_{\mathcal{T}_{i,m}}\right\|_{\mathbb{Y}_{i,m}} \longrightarrow 0$ as m goes to $+\infty$,
(iii) $(v_{\mathcal{T}_{i,m}})_{m\in\mathbb{N}}$ converges in $L^1(\Omega_i)$ to v_i.
Then, let us show that $(v_{\mathcal{T}_{i,m}})_{m\in\mathbb{N}}$ converges in fact to 0 in $L^1(\Omega_i)$. To this end, we consider a regular function φ on Ω_i. Let us set

$$\varphi_{\mathcal{D}_{i,m}} = \Big((\varphi(\mathbf{x}_K))_{K\in\mathcal{T}_{i,m}},\, (\varphi(\mathbf{x}_\sigma))_{\sigma\in\mathcal{F}_{i,m}\cup\mathcal{F}_{\Gamma,m}}\Big).$$

We first observe that

$$\begin{aligned}\left|\int_{\Omega_i} \phi_i v_{\mathcal{T}_{i,m}} \varphi_{\mathcal{T}_{i,m}}\,\mathrm{d}\mathbf{x}\right| &\leq C\left\|v_{\mathcal{T}_{i,m}}\right\|_{\mathbb{Y}_{i,m}} \left(\sum_{K\in\mathcal{T}_{i,m}}\sum_{\sigma\in\mathcal{F}_K}\frac{|\sigma|}{d_{K,\sigma}}(\varphi_K-\varphi_\sigma)^2\right)^{1/2}\\ &\leq C\left\|v_{\mathcal{T}_{i,m}}\right\|_{\mathbb{Y}_{i,m}}\|\nabla\varphi\|_{L^\infty} \longrightarrow 0.\end{aligned}$$

By virtue of (iii), the limit v_i of $(v_{\mathcal{T}_{i,m}})_{m\in\mathbb{N}}$ satisfies $\int_{\Omega_i}\phi_i v_i \varphi\,\mathrm{d}\mathbf{x} = 0$. This relation holds for any test function φ. Hence $\phi_i v_i = 0$. Assumption $(\mathbf{A}_1)$ yields $v_i = 0$, which concludes the proof. □

The next proposition states the boundedness of the sequence $(s_{\mathcal{T}_{i,m}})_{n\in\mathbb{N}}$ in $L^1(0, t_f; \mathcal{Y}_{i,m})$.

Proposition 4.3. *There exists C depending only on the data such that*

$$\sum_{n=1}^{N}\triangle t\left\|s^n_{\mathcal{T}_{i,m}}(\cdot+\mathbf{y}) - s^n_{\mathcal{T}_{i,m}}\right\|_{L^1(\Omega_i)} \leq C\,|\mathbf{y}|^{\Theta}, \quad \forall \mathbf{y}\in\mathbb{R}^d.$$

Consequently

$$\sum_{n=1}^{N}\triangle t\left\|s^n_{\mathcal{T}_{i,m}}\right\|_{\mathcal{Y}_{i,m}} \leq C.$$

Proof. By the inequality (2.15), one has

$$A_{i,\mathbf{y}}^n := \left\| s_{\mathcal{T}_{i,m}}^n(\cdot + \mathbf{y}) - s_{\mathcal{T}_{i,m}}^n \right\|_{L^1(\Omega_i)} \le L_c \int_{\Omega_i} \left| \xi_{\mathcal{T}_{i,m}}^n(\mathbf{x}+\mathbf{y}) - \xi_{\mathcal{T}_{i,m}}^n(\mathbf{x}) \right|^\Theta \mathrm{d}\mathbf{x}.$$

Applying Hölder's inequality leads to

$$A_{i,\mathbf{y}}^n \le C_\Theta \left(\int_{\Omega_i} \left| \xi_{\mathcal{T}_{i,m}}^n(\mathbf{x}+\mathbf{y}) - \xi_{\mathcal{T}_{i,m}}^n(\mathbf{x}) \right| \mathrm{d}\mathbf{x} \right)^\Theta .$$

Following [19, Lemma B.17], we infer

$$A_{i,\mathbf{y}}^n \le C'_\Theta \left| \mathbf{y} \right|^\Theta \left\| \xi_{\mathcal{D}_{i,m}}^n \right\|_{1,\mathcal{D}_{i,m}}^\Theta .$$

Applying once more the Hölder inequality and using the estimate (3.27), one obtains

$$\sum_{n=1}^N \triangle t A_{i,\mathbf{y}}^n \le C''_\Theta \left| \mathbf{y} \right|^\Theta \left(\sum_{n=1}^N \triangle t \left\| \xi_{\mathcal{D}_{i,m}}^n \right\|_{1,\mathcal{D}_{i,m}}^2 \right)^{\Theta/2} \le C'''_\Theta \left| \mathbf{y} \right|^\Theta ,$$

which implies the first inequality in the proposition. The proof of the second inequality is trivial since $s_{\mathcal{T}_{i,m}}^n$ is always bounded thanks to Lemma 3.5. This concludes the proof. $\square$

Let us next define the discrete time derivative $\delta_m s_{\mathcal{T}_{i,m}} : \Omega_i \times (0, t_f) \to \mathbb{R}$ such that its restriction on $K \times (t^{n-1}, t^n]$ is given by

$$(\delta_m s_{\mathcal{T}_{i,m}})_K^n = \frac{s_{\mathrm{rt}_K}(\pi_K^n) - s_{\mathrm{rt}_K}(\pi_K^{n-1})}{\triangle t}.$$

We also define

$$(\delta_m s_{\mathcal{T}_{i,m}})^n = \sum_{K \in \mathcal{T}_{i,m}} (\delta_m s_{\mathcal{T}_{i,m}})_K^n \mathbf{1}_K \in \mathbb{Y}_{i,m}.$$

The sequence of discrete time derivatives $(\delta_m s_{\mathcal{T}_{i,m}})_{n\in\mathbb{N}}$ verifies a uniform estimate in $L^1(0, t_f; \mathbb{Y}_{i,m})$. as claimed in the following result.

Proposition 4.4. *There exists C depending only on the data such that*

$$\sum_{n=1}^N \triangle t \left\| (\delta_m s_{\mathcal{T}_{i,m}})^n \right\|_{\mathbb{Y}_{i,m}} \le C.$$

Proof. Let $\psi_{\mathcal{D}_{i,m}} \in X_{i,m}^0$, adding the sum over $K \in \mathcal{T}_{i,m}$ of the non-wetting phase saturation conservation equation (3.3) multiplied by ψ_K and the sum over $\sigma \in \mathcal{F}_{i,m}$ of the non-wetting phase flux continuity equation (3.5) multiplied by ψ_σ, one obtains the equality

$$R_{1,i}^n = R_{2,i}^n + R_{3,i}^n,$$

where

$$R_{1,i}^n = \sum_{K \in \mathcal{T}_{i,m}} \phi_K \left| K \right| (\delta_m s_{\mathcal{T}_{i,m}})_K^n \psi_K = \int_{\Omega_i} \phi_i (\delta_m s_{\mathcal{T}_{i,m}})^n \psi_{\mathcal{T}_{i,m}} \,\mathrm{d}\mathbf{x},$$

$$R_{2,i}^n = - \sum_{K \in \mathcal{T}_{i,m}} \sum_{\sigma \in \mathcal{F}_K} \mathbb{T}_{K,\sigma} f_{\mathrm{rt}_K}^{\mathrm{nw}}(s_{K,\sigma}^{\mathrm{up},n}) M_{\mathrm{rt}_K}^T(c_{K,\sigma}^n)(P_K^n - P_{K,\sigma}^n)\Big(\psi_K - \psi_\sigma\Big),$$

$$R_{3,i}^n = - \sum_{K \in \mathcal{T}_m^i} \sum_{\sigma \in \mathcal{F}_K} \mathbb{T}_{K,\sigma} \eta_{K,\sigma}^n \Big(\pi_K^n - \pi_\sigma^n\Big)\Big(\psi_K - \psi_\sigma\Big),$$

where we have used (3.25) in $R^n_{2,i}$. Bearing in mind that the function f^{nw}_K is bounded, using the Cauchy-Schwarz inequality and Assumption $(\mathbf{A}_4)$, it results that

$$\left|R^n_{2,i}\right|^2 \leq C \left(\sum_{K\in\mathcal{T}_{i,m}} \sum_{\sigma\in\mathcal{F}_K} \mathbb{T}_{K,\sigma}(P^n_K - P^n_{K,\sigma})^2 \right) \left\|\psi_{\mathcal{D}_{i,m}}\right\|^2_{1,\mathcal{D}_{i,m}}.$$

In a similar way, one obtains the estimate

$$\left|R^n_{3,i}\right|^2 \leq C \left(\sum_{K\in\mathcal{T}_{i,m}} \sum_{\sigma\in\mathcal{F}_K} \mathbb{T}_{K,\sigma}\eta^n_{K,\sigma}\left(\pi^n_K - \pi^n_\sigma\right)^2 \right) \left\|\psi_{\mathcal{D}_{i,m}}\right\|^2_{1,\mathcal{D}_{i,m}}.$$

Moreover, taking the supremum of $R^n_{1,i} = R^n_{2,i} + R^n_{3,i}$ over all $\psi_{\mathcal{D}_{i,m}}$ such that $\left\|\psi_{\mathcal{D}_{i,m}}\right\|_{1,\mathcal{D}_{i,m}} \leq 1$ as in the definition of $\|\cdot\|_{\mathbb{Y}_{i,m}}$, we infer

$$\begin{aligned}\left\|(\delta_m s_{\mathcal{T}_{i,m}})^n\right\|_{\mathbb{Y}_{i,m}} \leq{}& C \left(\sum_{K\in\mathcal{T}_{i,m}} \sum_{\sigma\in\mathcal{F}_K} \mathbb{T}_{K,\sigma}(P^n_K - P^n_{K,\sigma})^2 \right)^{1/2} \\ &+ C \left(\sum_{K\in\mathcal{T}_{i,m}} \sum_{\sigma\in\mathcal{F}_K} \mathbb{T}_{K,\sigma}\eta^n_{K,\sigma}\left(\pi^n_K - \pi^n_\sigma\right)^2 \right)^{1/2}.\end{aligned}$$

Finally, summing over $n \in [\![1, N]\!]$, using again the Cauchy-Schwarz inequality and the energy estimates (3.26), (3.28), it results that

$$\begin{aligned}\sum_{n=1}^{N} \triangle t \left\|(\delta_m s_{\mathcal{T}_{i,m}})^n\right\|_{\mathbb{Y}_{i,m}} &\leq C \left(\sum_{n=1}^{N} \triangle t \sum_{K\in\mathcal{T}_m} \sum_{\sigma\in\mathcal{F}_K} \mathbb{T}_{K,\sigma}\Big((P^n_K - P^n_{K,\sigma})^2 + \eta^n_{K,\sigma}\left(\pi^n_K - \pi^n_\sigma\right)^2 \Big) \right)^{1/2} \\ &\leq C.\end{aligned}$$

The proof is thereby concluded. □

The following proposition states the convergence up to a subsequence of the finite volume scheme.

Proposition 4.5. *Let $(\mathcal{T}_{i,m}, \triangle t_m)_{m\in\mathbb{N}}$ be a sequence of discretizations of $Q^i_{t_f}$ such that $h_{\mathcal{T}_{i,m}}$ and $\triangle t_m$ go to zero as m tends to $+\infty$, and $\inf_{m\in\mathbb{N}} \zeta_{\mathcal{T}_m} > 0$. Let $(\pi_{\mathcal{T}_{i,m}}, p^{\mathrm{nw}}_{\mathcal{T}_{i,m}})_{m\in\mathbb{N}}$ be the corresponding sequence of discrete solutions to the finite volume scheme (3.3)-(3.7). Then, there exist $\pi_i \in L^2(Q^i_{t_f})$ with $\xi_i(\pi_i) \in L^2(0, t_f; H^1(\Omega))$, $p^\alpha_i \in L^2(Q^i_{t_f})$, and $P_i \in L^2(0, t_f; H^1(\Omega_i))$ such that $\pi_i = p^{\mathrm{nw}}_i - p^{\mathrm{w}}_i$ and, up to a subsequence as m tends to $+\infty$,*

$$s_{\mathcal{T}_{i,m}} \longrightarrow s_i(\pi_i) \qquad \textit{a.e. in } Q^i_{t_f} \textit{ and strongly in } L^1(Q^i_{t_f}), \tag{4.3}$$

$$F_i(\pi_{\mathcal{T}_{i,m}}) \longrightarrow F_i(\pi_i) \qquad \textit{strongly in } L^1(Q^i_{t_f}), \tag{4.4}$$

$$p^\alpha_{\mathcal{T}_{i,m}} \longrightarrow p^\alpha_i \qquad \textit{weakly } L^2(Q^i_{t_f}), \tag{4.5}$$

$$\nabla_{\mathcal{D}_{i,m}} F_i(\pi_{\mathcal{D}_{i,m}}) \longrightarrow \nabla F_i(\pi_i) \qquad \textit{weakly } L^2(Q^i_{t_f})^d, \tag{4.6}$$

$$\nabla_{\mathcal{D}_{i,m}} P_{\mathcal{D}_{i,m}} \longrightarrow \nabla P_i \qquad \textit{weakly } L^2(Q^i_{t_f})^d. \tag{4.7}$$

Proof. First, to prove that the saturation $s_{\mathcal{T}_{i,m}}$ converges strongly, we apply the discrete Aubin-Simon time compactness criterion elaborated in [19, Theorem C.8]. Let us hereafter summarize its main ingredients.

(a) $(\mathcal{Y}_{i,m}, \mathbb{Y}_{i,m})_{m\in\mathbb{N}}$ is compactly-continuously embedded in $L^1(\Omega_i)$, as shown in Proposition 4.2.

(b) The family $(s_{\mathcal{T}_{i,m}})_{m\in\mathbb{N}}$ is bounded in $L^1(0, t_f; L^1(\Omega_i))$, as stated in Proposition 4.3.

(c) The sequence $\left(\|s_{\mathcal{T}_{i,m}}\|_{L^1(0,t_f;\mathcal{Y}_{i,m})}\right)_{m\in\mathbb{N}}$ is bounded, which is provided by Proposition 4.3.

(d) The sequence $\left(\|\delta_m s_{\mathcal{T}_{i,m}}\|_{L^1(0,t_f;\mathbb{Y}_{i,m})}\right)_{m\in\mathbb{N}}$ is bounded, as established in Proposition 4.4.

Thanks to [19, Theorem C.8], the sequence $(s_{\mathcal{T}_{i,m}})_{m\in\mathbb{N}}$ is relatively compact in $L^1(Q^i_{t_f})$. Therefore there exists $\bar{s}_i \in L^1(Q^i_{t_f})$ such that, up to a subsequence,

$$s_{\mathcal{T}_{i,m}} \longrightarrow \bar{s}_i \quad \text{strongly in } L^1(Q^i_{t_f}) \text{ and a.e. on } Q^i_{t_f}.$$

Using Remark 3.6 stating that $\pi_{\mathcal{T}_{i,m}} \in [\underline{\pi}_i, \overline{\pi}_i]$ and Assumption $(\mathbf{A}_2)$, we can define $s_i^{-1} : [0,1] \to [\underline{\pi}_i, \overline{\pi}_i]$, the continuous inverse of s_i. Then, there exists a subsequence of $(\pi_{\mathcal{T}_{i,m}})_{m\in\mathbb{N}}$, still denoted by $(\pi_{\mathcal{T}_{i,m}})_{m\in\mathbb{N}}$ for convenience, such that

$$\pi_{\mathcal{T}_{i,m}} \longrightarrow \pi_i := s_i^{-1}(\bar{s}_i) \quad \text{a.e. in } Q^i_{t_f},$$

According to the uniform bounds on the discrete capillary pressure $\pi_{\mathcal{T}_{i,m}}$ established in Lemma 3.5, we obtain, for all $r \geq 1$, that

$$\omega(\pi_{\mathcal{T}_{i,m}}) \longrightarrow \omega(\pi_i) \quad \text{strongly in } L^r(Q^i_{t_f}), \quad \text{with} \quad \omega = F_i, \xi_i. \tag{4.8}$$

Next, let us show the weak convergence (4.6) of the discrete gradient. First, by virtue of Proposition 3.7, it can be checked that

$$\|\nabla_{\mathcal{D}_{i,m}} F_i(\pi_{\mathcal{D}_{i,m}})\|_{L^2(Q^i_{t_f})^d} = \sum_{n=1}^{N} \triangle t \sum_{K\in\mathcal{T}_{i,m}} \sum_{\sigma\in\mathcal{F}_K} \frac{|\sigma|}{d_{K,\sigma}} \Big(F_{\mathrm{rt}_K}(\pi^n_K) - F_{\mathrm{rt}_K}(\pi^n_\sigma)\Big)^2 \leq C. \tag{4.9}$$

Thus, there exists $\Psi \in L^2(Q^i_{t_f})^d$ such that $\nabla_{\mathcal{D}_{i,m}} F_i(\pi_{\mathcal{D}_{i,m}})$ converges weakly towards Ψ. The proof of $\Psi = \nabla F_i(\pi_i)$ is classical. It uses the proof guidelines of [24, Lemma 4.3]. Similarly, one can check that $\nabla_{\mathcal{D}_{i,m}} \xi_i(\pi_{\mathcal{D}_{i,m}})$ converges weakly towards $\nabla\xi_i(\pi_i)$ with $\xi_i(\pi_i) \in L^2(0,t_f;H^1(\Omega))$. An analogous argument can be employed to prove (4.7). This concludes the proof. $\square$

4.2 Passage to the limit in the scheme

Let $(\mathbf{t}^j_\sigma)_{j\in\{1,\cdots,d-1\}}$ with $\mathbf{t}^j_\sigma \in \mathbb{R}^d$ be an orthonormal basis of σ. Let ψ be a smooth function, we define its interpolant on $X_{i,m}$ by

$$\psi^n_{\mathcal{D}_{i,m}} = \mathfrak{T}^n_{\mathcal{D}_{i,m}}\psi := \Big((\psi(\mathbf{x}_K, t^n))_{K\in\mathcal{T}_{i,m}}, (\psi(\mathbf{x}_\sigma, t^n))_{\sigma\in\mathcal{F}_{i,m}\cup\mathcal{F}_{\Gamma,m}}\Big).$$

Following [18], a consistent approximate gradient of ψ is defined by

$$\widehat{\nabla}_{\mathcal{D}_{i,m}}\psi_{\mathcal{D}_{i,m}}(\mathbf{x},t) = \frac{\psi^n_\sigma - \psi^n_K}{d_{K,\sigma}}\mathbf{n}_{K,\sigma} + \sum_{j=1}^{d-1}\Big(\nabla\psi(\mathbf{x}_\sigma, t^n)\cdot\mathbf{t}^j_\sigma\Big)\mathbf{t}^j_\sigma, \quad (\mathbf{x},t) \in D_{K,\sigma}\times(t^{n-1},t^n].$$

Using that $|D_{K,\sigma}| = \frac{|\sigma| d_{K,\sigma}}{d}$, it can be checked that

$$\int_{Q^i_{t_f}} \nabla_{\mathcal{D}_{i,m}} u_{\mathcal{D}_{i,m}} \cdot \widehat{\nabla}_{\mathcal{D}_{i,m}}\psi_{\mathcal{D}_{i,m}} \,\mathrm{d}\mathbf{x}\,\mathrm{d}t = \sum_{n=1}^{N} \triangle t \sum_{K\in\mathcal{T}_{i,m}} \sum_{\sigma\in\mathcal{F}_K} \frac{|\sigma|}{d_{K,\sigma}} \big(u^n_{K,\sigma} - u^n_\sigma\big)\big(\psi^n_K - \psi^n_\sigma\big).$$

The following proposition establishes that the limit functions $(\pi_i, P_i)_{i\in\{1,2\}}$ of Proposition 4.5 satisfy the variational formulation (2.18)-(2.19). The transmission conditions (2.16)-(2.17) are shown to be verified in the next subsection.

Proposition 4.6. *The functions $(\pi_i, P_i)_{i\in\{1,2\}}$ satisfy the variational formulation (2.18)-(2.19) given in Definition 2.1.*

Proof. Let us select φ a smooth function in $\mathcal{C}_c^\infty(\overline{\Omega}\times[0,t_f))$ and define, for $i\in\{1,2\}$, the interpolant $\varphi^n_{\mathcal{D}_{i,m}} = \mathfrak{T}^n_{\mathcal{D}_{i,m}}\varphi$. Adding the sum over $K\in\mathcal{T}_m$ of equation (3.3) multiplied by $\triangle t\ \varphi^n_K$ and the sum over $\sigma\in\mathcal{F}_m$ of equation (3.5) multiplied by $\triangle t\ \varphi^n_\sigma$, summing over $n\in[\![1,N]\!]$, one obtains that

$$A_m + B_m + C_m = 0,$$

with

$$\begin{aligned}
A_m &= \sum_{n=1}^N \sum_{K\in\mathcal{T}_m} \phi_K\,|K|\left(s_{\mathrm{rt}_K}(\pi^n_K) - s_{\mathrm{rt}_K}(\pi^{n-1}_K)\right)\varphi^n_K,\\
B_m &= \sum_{n=1}^N \triangle t \sum_{K\in\mathcal{T}_m}\sum_{\sigma\in\mathcal{F}_K} \mathbb{T}_{K,\sigma} f^{\mathrm{nw}}_{\mathrm{rt}_K}(s^{\mathrm{up},n}_{K,\sigma}) M^T_{\mathrm{rt}_K}(c^n_{K,\sigma})(P^n_K - P^n_{K,\sigma})(\varphi^n_K-\varphi^n_\sigma),\\
C_m &= \sum_{n=1}^N \triangle t \sum_{K\in\mathcal{T}_m}\sum_{\sigma\in\mathcal{F}_K} \mathbb{T}_{K,\sigma}\eta^n_{K,\sigma}(\pi^n_K-\pi^n_\sigma)(\varphi^n_K-\varphi^n_\sigma).
\end{aligned}$$

Applying a discrete integration-by-parts (see [19, Section D.1.7]) to A_m gives

$$\begin{aligned}
A_m &= -\sum_{n=1}^N\sum_{K\in\mathcal{T}_m}\phi_K\,|K|\,s_{\mathrm{rt}_K}(\pi^{n-1}_K)\left(\varphi^n_K-\varphi^{n-1}_K\right) - \sum_{K\in\mathcal{T}_m}\phi_K\,|K|\,s_{\mathrm{rt}_K}(\pi^0_K)\varphi^0_K,\\
&= -\sum_{i\in\{1,2\}}\left(\int_{Q^i_{t_f}}\phi_i s_{\mathcal{T}_{i,m}}(\cdot,\cdot-\triangle t)\delta_m\varphi_{\mathcal{T}_{i,m}}\,\mathrm{d}\mathbf{x}\,\mathrm{d}t + \int_{\Omega_i}\phi_i s_i(\pi^0_{\mathcal{T}_{i,m}})\varphi(\cdot,0)\,\mathrm{d}\mathbf{x}\right).
\end{aligned}$$

Note that the function $s_{\mathcal{T}_{i,m}}$ is extended by $s_i(\pi^0_{\mathcal{T}_{i,m}})$ for negative times. Thanks to the strong convergence (4.3) and to the uniform convergence of $\delta_m\varphi_{\mathcal{T}_{i,m}}$ towards $\partial_t\varphi_i$, we infer

$$A_m \longrightarrow -\sum_{i=1,2}\left(\int_{Q^i_{t_f}}\phi s_i(\pi_i)\partial_t\varphi\,\mathrm{d}\mathbf{x}\,\mathrm{d}t + \int_{\Omega_i}\phi s_i(\pi^0_i)\varphi(\cdot,0)\,\mathrm{d}\mathbf{x}\right).$$

Let us define $\Lambda_{\mathcal{T}_{i,m}} = \sum_{K\in\mathcal{T}_{i,m}}\Lambda_K\mathbf{1}_K$. It can be checked that $\Lambda_{\mathcal{T}_{i,m}}\to\Lambda$ a.e. in $\Omega\times(0,t_f)$. Assumption ($\mathbf{A}_5$) and Hölder's inequality ensure that

$$\begin{aligned}
W_{i,m} &:= \int_{Q^i_{t_f}}\left|s_i(\pi_{\mathcal{T}_{i,m}}) - s_i(\Pi_{\mathcal{D}_{i,m}}\pi_{\mathcal{D}_{i,m}})\right|^2\mathrm{d}\mathbf{x}\,\mathrm{d}t\\
&\le C\int_{Q^i_{t_f}}\left|\xi_i(\pi_{\mathcal{T}_{i,m}}) - \xi_i(\Pi_{\mathcal{D}_{i,m}}\pi_{\mathcal{D}_{i,m}})\right|^{2\Theta}\mathrm{d}\mathbf{x}\,\mathrm{d}t\\
&\le C\left|Q^i_{t_f}\right|^{1-\Theta}\left(\int_{Q^i_{t_f}}\left|\xi_i(\pi_{\mathcal{T}_{i,m}}) - \xi_i(\Pi_{\mathcal{D}_{i,m}}\pi_{\mathcal{D}_{i,m}})\right|^2\mathrm{d}\mathbf{x}\,\mathrm{d}t\right)^\Theta\\
&\le Ch^{2\Theta}_{\mathcal{T}_m}\left\|\nabla_{\mathcal{D}_{i,m}}\xi_i(\pi_{\mathcal{D}_{i,m}})\right\|^{2\Theta}_{L^2(Q^i_{t_f})^d}.
\end{aligned}\tag{4.10}$$

The last inequality is obtained by first developing the integral in (4.10) into $\sum_{K\in\mathcal{T}_m}\sum_{\sigma\in\mathcal{F}_K}\int_{D_{K,\sigma}}$, and then by introducing the definition of the two-point discrete gradient and the fact that $|D_{K,\sigma}| = \frac{|\sigma|d_{K,\sigma}}{d}$ to conclude. Observing that

$$\left\|\nabla_{\mathcal{D}_{i,m}}\xi_i(\pi_{\mathcal{D}_{i,m}})\right\|^2_{L^2(Q^i_{t_f})^d} \le \frac{1}{\underline{\Lambda}}\sum_{n=1}^N\triangle t\left\|\xi_i(\pi^n_{\mathcal{D}_{i,m}})\right\|^2_{1,\mathcal{D}_{i,m}},$$

the energy estimate (3.27) shows that $W_{i,m}\le Ch^{2\Theta}_{\mathcal{T}_m}$. The strong convergence (4.3) then yields

$$s_i(\Pi_{\mathcal{D}_{i,m}}\pi_{\mathcal{D}_{i,m}}) \longrightarrow s_i(\pi_i)\quad \text{a.e. in } Q^i_{t_f} \text{ and strongly in } L^2(Q^i_{t_f}).\tag{4.11}$$

As a consequence, the weak convergence (4.7) and the uniform convergence of $\widehat{\nabla}_{\mathcal{D}_{i,m}}\varphi_{\mathcal{D}_{i,m}}$ towards $\nabla\varphi$ give

$$B'_m := \sum_{i\in\{1,2\}}\int_{Q^i_{t_f}} f_i^{\mathrm{nw}}\big(s_i(\Pi_{\mathcal{D}_{i,m}}\pi_{\mathcal{D}_{i,m}})\big)M_i^T\big(s_i(\Pi_{\mathcal{D}_{i,m}}\pi_{\mathcal{D}_{i,m}})\big)\Lambda_{\mathcal{T}_{i,m}}\nabla_{\mathcal{D}_{i,m}}P_{\mathcal{D}_{i,m}}\cdot\widehat{\nabla}_{\mathcal{D}_{i,m}}\varphi_{\mathcal{D}_{i,m}}\,\mathrm{d}\mathbf{x}\,\mathrm{d}t$$
$$\longrightarrow \sum_{i\in\{1,2\}}\int_{Q^i_{t_f}} M_i^{\mathrm{nw}}\big(s_i(\pi_i)\big)\Lambda\nabla P_i\cdot\nabla\varphi\,\mathrm{d}\mathbf{x}\,\mathrm{d}t.$$

It is subsequently shown that B_m and B'_m tend to the same limit. For shortness, let us set $w^n_{K,\sigma}=w_{\mathrm{rt}_K}(\pi^n_\sigma)$, and $w^n_K=w_{\mathrm{rt}_K}(\pi^n_K)$, for $w=s,\xi$. We observe that

$$\big|B_m-B'_m\big|\le\sum_{n=1}^N\triangle t\sum_{K\in\mathcal{T}_m}\sum_{\sigma\in\mathcal{F}_K}\mathbb{T}_{K,\sigma}\Bigg(\Big|f^{\mathrm{nw}}_{\mathrm{rt}_K}(s^n_K)-f^{\mathrm{nw}}_{\mathrm{rt}_K}(s^n_{K,\sigma})\Big|\,M^T_{\mathrm{rt}_K}(c^n_{K,\sigma})$$
$$+\Big|M^T_{\mathrm{rt}_K}(c^n_{K,\sigma})-M^T_{\mathrm{rt}_K}(s^n_{K,\sigma})\Big|\,f^{\mathrm{nw}}_{\mathrm{rt}_K}(s^n_{K,\sigma})\Bigg)\,\big|P^n_K-P^n_{K,\sigma}\big|\,\big|\varphi^n_K-\varphi^n_\sigma\big|\,.$$

Now, Assumption $(\mathbf{A}_3)$ implies

$$\Big|f^{\mathrm{nw}}_{\mathrm{rt}_K}(s^n_K)-f^{\mathrm{nw}}_{\mathrm{rt}_K}(s^n_{K,\sigma})\Big|\,M^T_{\mathrm{rt}_K}(c^n_{K,\sigma})+\Big|M^T_{\mathrm{rt}_K}(c^n_{K,\sigma})-M^T_{\mathrm{rt}_K}(s^n_{K,\sigma})\Big|\,f^{\mathrm{nw}}_{\mathrm{rt}_K}(s^n_{K,\sigma})$$
$$\le C\Big(\Big|M^{\mathrm{nw}}_{\mathrm{rt}_K}(s^n_K)-M^{\mathrm{nw}}_{\mathrm{rt}_K}(s^n_{K,\sigma})\Big|+\Big|M^{\mathrm{w}}_{\mathrm{rt}_K}(s^n_K)-M^{\mathrm{w}}_{\mathrm{rt}_K}(s^n_{K,\sigma})\Big|\Big).$$

By virtue of the Cauchy-Schwarz inequality, the estimation (3.28), the previous estimate and (4.11), it results that

$$\big|B_m-B'_m\big|\le C_\varphi\left(\sum_{n=1}^N\triangle t\sum_{K\in\mathcal{T}_m}\sum_{\sigma\in\mathcal{F}_K}\mathbb{T}_{K,\sigma}\big|P^n_K-P^n_{K,\sigma}\big|^2\right)^{1/2}$$
$$\times\left(\sum_{\alpha\in\{\mathrm{nw},\mathrm{w}\}}\sum_{n=1}^N\triangle t\sum_{K\in\mathcal{T}_m}\sum_{\sigma\in\mathcal{F}_K}|D_{K,\sigma}|\Big(M^\alpha_{\mathrm{rt}_K}(s^n_K)-M^\alpha_{\mathrm{rt}_K}(s^n_{K,\sigma})\Big)^2\right)^{1/2}$$
$$\le C\sum_{i\in\{1,2\}}\left(\sum_{\alpha\in\{\mathrm{nw},\mathrm{w}\}}\big\|M_i^\alpha\big(s_i(\pi_{\mathcal{T}_{i,m}})\big)-M_i^\alpha\big(s_i(\Pi_{\mathcal{D}_{i,m}}\pi_{\mathcal{D}_{i,m}})\big)\big\|^2_{L^2(Q^i_{t_f})}\right)^{1/2}\longrightarrow 0.$$

Let us finally establish the convergence of the capillary term. First, for every $\sigma\in\mathcal{F}$, there exists $u^n_{K,\sigma}\in[\pi^\star,\pi^{\star\star}]$ such that, setting $y^n_{K,\sigma}:=s_{\mathrm{rt}_K}(u^n_{K,\sigma})$,

$$F_{\mathrm{rt}_K}(\pi^n_K)-F_{\mathrm{rt}_K}(\pi^n_\sigma)=\sqrt{\eta_{\mathrm{rt}_K}(y^n_{K,\sigma})}\big(\xi_{\mathrm{rt}_K}(\pi_K)-\xi_{\mathrm{rt}_K}(\pi^n_\sigma)\big).$$

As a consequence of (4.6) we get

$$\mathcal{C}'_m:=\sum_{n=1}^N\triangle t\sum_{K\in\mathcal{T}_m}\sum_{\sigma\in\mathcal{F}_K}\mathbb{T}_{K,\sigma}\sqrt{\eta_{\mathrm{rt}_K}(y^n_{K,\sigma})}(\xi^n_K-\xi^n_{K,\sigma})(\varphi^n_K-\varphi^n_\sigma)$$
$$=\sum_{i\in\{1,2\}}\int_{Q^i_{t_f}}\Lambda_{\mathcal{T}_{i,m}}\nabla_{\mathcal{D}_{i,m}}F_i(\pi_{\mathcal{D}_{i,m}})\cdot\widehat{\nabla}_{\mathcal{D}_{i,m}}\varphi_{\mathcal{D}_{i,m}}\,\mathrm{d}\mathbf{x}\,\mathrm{d}t\longrightarrow\sum_{i\in\{1,2\}}\int_{Q^i_{t_f}}\Lambda\nabla F_i(\pi_i)\cdot\nabla\varphi\,\mathrm{d}\mathbf{x}\,\mathrm{d}t.$$

On the other hand, let us reformulate $\mathcal{C}'_m$ as follows

$$\mathcal{C}'_m=\sum_{n=1}^N\triangle t\sum_{K\in\mathcal{T}_m}\sum_{\sigma\in\mathcal{F}_K}\mathbb{T}_{K,\sigma}\sqrt{\eta_{\mathrm{rt}_K}(y^n_{K,\sigma})}\sqrt{\eta_{\mathrm{rt}_K}(z^n_{K,\sigma})}(\pi^n_K-\pi^n_\sigma)(\varphi^n_K-\varphi^n_\sigma),$$

where $z_{K,\sigma}$ is given by

$$\eta_{\mathrm{rt}_K}(z^n_{K,\sigma}) = \begin{cases} \left(\dfrac{\xi^n_K - \xi^n_{K,\sigma}}{\pi^n_K - \pi^n_\sigma}\right)^2 & \text{if } \pi^n_K \neq \pi^n_\sigma \\ \eta_{\mathrm{rt}_K}(\pi^n_K) & \text{otherwise.} \end{cases}$$

In addition, setting

$$\mathcal{C}''_m := \sum_{n=1}^{N} \triangle t \sum_{K\in\mathcal{T}_m} \sum_{\sigma\in\mathcal{F}_K} \mathbb{T}_{K,\sigma} \sqrt{\eta_{\mathrm{rt}_K}(y^n_{K,\sigma})} \sqrt{\eta^n_{K,\sigma}} (\pi^n_K - \pi^n_\sigma)(\varphi^n_K - \varphi^n_\sigma),$$

it results that

$$\begin{aligned} |\mathcal{C}_m - \mathcal{C}''_m| &\leq C_\varphi \sum_{n=1}^{N} \triangle t \sum_{K\in\mathcal{T}_m} \sum_{\sigma\in\mathcal{F}_K} \mathbb{T}_{K,\sigma} d_{K,\sigma} \left| \sqrt{\eta_{\mathrm{rt}_K}(y^n_{K,\sigma})} - \sqrt{\eta^n_{K,\sigma}} \right| \sqrt{\eta^n_{K,\sigma}} \, |\pi^n_K - \pi^n_\sigma| \\ &\leq C \left(\sum_{n=1}^{N} \triangle t \sum_{K\in\mathcal{T}_m} \sum_{\sigma\in\mathcal{F}_K} \mathbb{T}_{K,\sigma} \eta^n_{K,\sigma} \, |\pi^n_K - \pi^n_\sigma|^2 \right)^{1/2} \\ &\quad \times \left(\sum_{n=1}^{N} \triangle t \sum_{K\in\mathcal{T}_m} \sum_{\sigma\in\mathcal{F}_K} |D_{K,\sigma}| \left(\sqrt{\eta_{\mathrm{rt}_K}(y^n_{K,\sigma})} - \sqrt{\eta^n_{K,\sigma}} \right)^2 \right)^{1/2} \\ &\leq C \left(\sum_{n=1}^{N} \triangle t \sum_{K\in\mathcal{T}_m} \sum_{\sigma\in\mathcal{F}_K} |D_{K,\sigma}| \left(\sqrt{\eta_{\mathrm{rt}_K}(y^n_{K,\sigma})} - \sqrt{\eta^n_{K,\sigma}} \right)^2 \right)^{1/2}, \end{aligned}$$

where the Cauchy-Schwarz inequality is used in the second line, and the a priori estimate (3.26) in the last one. Moreover, the definition of the capillary diffusion function η_i ensures the existence of a positive constant C such that

$$\begin{aligned} &\left| \sqrt{\eta_{\mathrm{rt}_K}(y^n_{K,\sigma})} - \sqrt{\eta^n_{K,\sigma}} \right| \\ &\qquad \leq C \left(\left| \sqrt{M^{\mathrm{nw}}_{\mathrm{rt}_K}(s^n_K)} - \sqrt{M^{\mathrm{nw}}_{\mathrm{rt}_K}(s^n_{K,\sigma})} \right| + \left| \sqrt{M^{\mathrm{w}}_{\mathrm{rt}_K}(s^n_K)} - \sqrt{M^{\mathrm{w}}_{\mathrm{rt}_K}(s^n_{K,\sigma})} \right| \right). \end{aligned}$$

Following the same steps as for the convergence of the transport term, one deduces that

$$|\mathcal{C}_m - \mathcal{C}''_m| \longrightarrow 0.$$

Similarly, one obtains the following estimate

$$|\mathcal{C}'_m - \mathcal{C}''_m| \leq C_\varphi \sum_{n=1}^{N} \triangle t \sum_{K\in\mathcal{T}_m} \sum_{\sigma\in\mathcal{F}_K} \mathbb{T}_{K,\sigma} d_{K,\sigma} \left| \sqrt{\eta_{\mathrm{rt}_K}(z^n_{K,\sigma})} - \sqrt{\eta^n_{K,\sigma}} \right| \sqrt{\eta_{\mathrm{rt}_K}(y^n_{K,\sigma})} \, |\pi^n_K - \pi^n_\sigma| \, .$$

Thanks to (3.13), there exists $C > 0$ such that $\eta_{\mathrm{rt}_K}(y^n_{K,\sigma}) \leq C\eta^n_{K,\sigma}$. Therefore

$$|\mathcal{C}'_m - \mathcal{C}''_m| \leq C \sum_{n=1}^{N} \triangle t \sum_{K\in\mathcal{T}_m} \sum_{\sigma\in\mathcal{F}_K} \mathbb{T}_{K,\sigma} d_{K,\sigma} \left| \sqrt{\eta_{\mathrm{rt}_K}(z^n_{K,\sigma})} - \sqrt{\eta^n_{K,\sigma}} \right| \sqrt{\eta^n_{K,\sigma}} \, |\pi^n_K - \pi^n_\sigma| \, .$$

Proceeding as in the convergence of $|\mathcal{C}_m - \mathcal{C}''_m|$ it can be shown that

$$|\mathcal{C}'_m - \mathcal{C}''_m| \longrightarrow 0.$$

Finally, the passage to the limit in the discrete pressure equation follows similarly as done for B_m. This concludes the proof of Proposition 4.6. $\square$

4.3 Convergence of the discrete trace functions

In this section we prove that the functions $(\pi_i, P_i)_{i\in\{1,2\}}$ satisfy the transmission conditions (2.16) and (2.17). For a given vector $u_{\mathcal{D}_i} = (u^n_{\mathcal{D}_i})_{n\in[\![1,N]\!]} \in (X_i)^N$, let us define the one-sided trace Γ by

$$\gamma_{\mathcal{D}_i}(u_{\mathcal{D}_i})(\mathbf{x},t) = u^n_{K,\sigma}, \quad (\mathbf{x},t) \in \sigma \times (t^{n-1}, t^n], \quad \sigma \in \mathcal{F}_\Gamma, \quad \{K\} = \mathcal{T}_\sigma \cap \mathcal{T}_i.$$

light of (4.4)t he sequence $(F_i(\pi_{\mathcal{D}_{i,m}}))_{m\in\mathbb{N}}$ converges strongly up to a subsequence towards $F_i(\pi_i)$ which belongs to $L^2(0,t_f;H^1(\Omega_i))$. As a result, the trace of $F_i(\pi_i)$ denoted by $\gamma_i F_i(\pi_i)$ exists in the space $L^2(\Gamma\times(0,t_f))$. The first objective of the arguments presented below is to show that the sequence $(\gamma_{\mathcal{D}_{i,m}}(F_i(\pi_{\mathcal{D}_{i,m}})))_{m\in\mathbb{N}}$ tends up to a subsequence to $\gamma_i F_i(\pi_i)$ strongly in $L^1(\Gamma\times(0,t_f))$. To this end, we need to make use of another discrete trace function given by

$$\widehat{\gamma}_{\mathcal{D}_i}(u_{\mathcal{D}_i})(\mathbf{x},t) = u^n_K, \quad (\mathbf{x},t) \in \sigma \times (t^{n-1}, t^n], \quad \sigma \in \mathcal{F}_\Gamma, \quad \{K\} = \mathcal{T}_\sigma \cap \mathcal{T}_i.$$

The following result states that both definitions of the discrete trace have the same asymptotic behavior on the functions having bounded energy estimation. More importantly, it relates the interface solution to the whole approximate function in the overall domain. See [7, Lemma 4.7] for more details on the proof.

Lemma 4.7. *For any family $u_{\mathcal{D}_i} = (u^n_{\mathcal{D}_i})_{n\in[\![1,N]\!]} \in (X_i)^N$, one has*

$$\int_{\Gamma\times(0,t_f)} |\widehat{\gamma}_{\mathcal{D}_i}(u_{\mathcal{D}_i}) - \gamma_{\mathcal{D}_i}(u_{\mathcal{D}_i})| \,\mathrm{d}\sigma(\boldsymbol{x})\,\mathrm{d}t \le \|\nabla_{\mathcal{D}_i} u_{\mathcal{D}_i}\|_{L^2(Q^i_{t_f})^d} \,(|\Gamma|\, t_f h_{\mathcal{T}})^{1/2}.$$

The proposition below enables the strong convergence on the discrete trace of the Kirchhoff function F_i.

Proposition 4.8. *By extraction of a subsequence, the sequence $(\gamma_{\mathcal{D}_{i,m}}(F_i(\pi_{\mathcal{D}_{i,m}})))_{m\in\mathbb{N}}$ converges to $\gamma_i F_i(\pi_i)$ strongly in the sense of $L^1(\Gamma\times(0,t_f))$-norm.*

Proof. The proof is already provided in [7, Proposition 4.9]. It makes use of the boundedness of $F_i(\pi_{\mathcal{D}_{i,m}})$ (in L^∞ norm) which holds due to Lemma 3.5. An alternative and more general proof can be given based on the Discrete Functional Analysis tools from [19].

For $i\in\{1,2\}$, let $(u_{\mathcal{D}_{i,m}})_{m\in\mathbb{N}}$, with $u_{\mathcal{D}_{i,m}} \in (X_{i,m})^{N_m}$ for all $m\in\mathbb{N}$, be a sequence such that

$$\sum_{m\in\mathbb{N}} \int_0^{t_f} \|u_{\mathcal{D}_{i,m}}\|_{1,\mathcal{D}_{i,m}} \,\mathrm{d}t < +\infty$$

and $\Pi_{\mathcal{T}_{i,m}} u_{\mathcal{D}_{i,m}}$ converges strongly in $L^2(Q^i_{t_f})$ towards some $u_i \in L^2(0,t_f;H^1(\Omega_i))$. Let us denote by $\mathcal{I}_{i,m}$ the interpolation operator from $L^2(0,t_f;H^1(\Omega_i))$ to $(X_{i,m})^{N_m}$ defined by

$$(\mathcal{I}_{i,m} u_i)^n_K = \frac{1}{|K|\Delta t} \int_{t^{n-1}}^{t^n} \int_K u_i \,\mathrm{d}\mathbf{x}\,\mathrm{d}t \quad \text{for all } K\in\mathcal{T}_{i,m} \text{ and } n = 1,\dots,N,$$

and

$$(\mathcal{I}_{i,m} u_i)^n_\sigma = \frac{1}{|\sigma|\Delta t} \int_{t^{n-1}}^{t^n} \int_\sigma u_i \,\mathrm{d}\sigma(\mathbf{x})\,\mathrm{d}t \quad \text{for all } \sigma\in\mathcal{F}_{i,m} \text{ and } n = 1,\dots,N.$$

We have

$$\begin{aligned}
&\int_0^{t_f} \|\gamma_{\mathcal{D}_{i,m}} u_{\mathcal{D}_{i,m}} - \gamma_i u_i\|^2_{L^2(\Gamma)} \,\mathrm{d}t \\
&\quad \le 2\int_0^{t_f} \|\gamma_{\mathcal{D}_{i,m}} u_{\mathcal{D}_{i,m}} - \gamma_{\mathcal{D}_{i,m}} \mathcal{I}_{i,m} u_i\|^2_{L^2(\Gamma)} \,\mathrm{d}t + 2\int_0^{t_f} \|\gamma_{\mathcal{D}_{i,m}} \mathcal{I}_{i,m} u_i - \gamma_i u_i\|^2_{L^2(\Gamma)} \,\mathrm{d}t.
\end{aligned} \tag{4.12}$$

In order to prove that the right-hand-side of (4.12) tends to zero as $m \to \infty$ we make use of Proposition B.7, Proposition B.9 and Lemma B.21 from [19]. The adaptation of those results to our time dependent problem is straightforward.

In view of Proposition B.9, the second term in the right-hand-side of (4.12) tends to zero, while, using Lemma B.21 (with $p = 2$) we can estimate the first term as

$$\int_0^{t_f} \|\gamma_{\mathcal{D}_{i,m}} u_{\mathcal{D}_{i,m}} - \gamma_{\mathcal{D}_{i,m}} \mathcal{I}_{i,m} u_i\|^2_{L^2(\Gamma)} \,\mathrm{d}t \le C \left(T^1_m + T^2_m + T^3_m\right),$$

where

$$\begin{aligned} T^1_m &= \int_0^{t_f} \|u_{\mathcal{D}_{i,m}} - \mathcal{I}_{i,m} u_i\|_{1,\mathcal{D}_{i,m}} \|\Pi_{\mathcal{T}_{i,m}} u_{\mathcal{D}_{i,m}} - \Pi_{\mathcal{T}_{i,m}} \mathcal{I}_{i,m} u_i\|_{L^2(\Omega_i)} \,\mathrm{d}t, \\ T^2_m &= \int_0^{t_f} \|\Pi_{\mathcal{T}_{i,m}} u_{\mathcal{D}_{i,m}} - \Pi_{\mathcal{T}_{i,m}} \mathcal{I}_{i,m} u_i\|^2_{L^2(\Omega_i)} \,\mathrm{d}t, \\ T^3_m &= h_{\mathcal{T}_m} \int_0^{t_f} \|u_{\mathcal{D}_{i,m}} - \mathcal{I}_{i,m} u_i\|^2_{1,\mathcal{D}_{i,m}} \,\mathrm{d}t, \end{aligned}$$

and C is a constant depending only on Ω_i, d and ζ_0. From Proposition B.7 we deduce that the sequence $\int_0^{t_f} \|u_{\mathcal{D}_{i,m}} - \mathcal{I}_{i,m} u\|^2_{1,\mathcal{D}_{i,m}} \,\mathrm{d}t$ is bounded, and therefore $\lim\limits_{m\to\infty} T^3_m = 0$. In addition in view of Proposition B.9 we have $\int_0^{t_f} \|\Pi_{\mathcal{T}_{i,m}} u_{\mathcal{D}_{i,m}} - \Pi_{\mathcal{T}_m} \mathcal{I}_{i,m} u\|^2_{L^2(\Omega_i)} \,\mathrm{d}t \to 0$ as $m \to \infty$, which implies that T^1_m and T^2_m tend to zero and conclude the proof. □

Analogously, this fact holds true in the weak sense for the global pressure. The proof of this result can be found in [19] or [7].

Proposition 4.9. *Up to a subsequence, the sequence of discrete traces of the global pressures* $(\gamma_{\mathcal{D}_{i,m}}(P_{\mathcal{D}_{i,m}}))_{m\in\mathbb{N}}$ *converges to* $\gamma_i P_i$ *weakly in* $L^2(\Gamma \times (0, t_f))$.

Let us define $\pi_{\Gamma,\mathcal{D}_m}$ as follows

$$\pi_{\Gamma,\mathcal{D}_m}(\mathbf{x}, t) := \gamma_{\mathcal{D}_{m,1}}(\pi_{\mathcal{D}_{m,1}})(\mathbf{x}, t) := \pi^n_\sigma, \quad (\mathbf{x}, t) \in \sigma \times (t^{n-1}, t^n]$$

for all $\sigma \in \mathcal{F}_{\Gamma,m}$ and $n \in \{1, \ldots, N\}$. Note that $\gamma_{\mathcal{D}_{m,1}}(\pi_{\mathcal{D}_{m,1}}) = \gamma_{\mathcal{D}_{m,2}}(\pi_{\mathcal{D}_{m,2}})$. In addition $\pi_{\Gamma,\mathcal{D}_m}$ belongs to $[\pi^\star, \pi^{\star\star}]$ and therefore there exists a measurable function π_Γ defined a.e. on $\Gamma \times (0, t_f)$ such that, up to a subsequence,

$$\pi_{\Gamma,\mathcal{D}_m} \longrightarrow \pi_\Gamma \quad \text{weakly in } L^2(\Gamma \times (0, t_f)). \tag{4.13}$$

We have the following result.

Proposition 4.10. *The function* π_Γ *satisfies*

$$F_i(\pi_\Gamma) = \gamma_i F_i(\pi_i), \tag{4.14}$$

$$G^\alpha_i(\pi_{\Gamma,\mathcal{D}_m}) \longrightarrow G^\alpha_i(\pi_\Gamma) \quad \textit{weakly in } L^2(\Gamma \times (0, t_f)) \textit{ up to a subsequence.} \tag{4.15}$$

Proof. Notice that $F_i(\pi_{\Gamma,\mathcal{D}_m}) = \gamma_{\mathcal{D}_{i,m}} F_i(\pi_{\mathcal{D}_{i,m}})$, and by virtue of Proposition 4.8, we have

$$\gamma_{\mathcal{D}_{i,m}} F_i(\pi_{\mathcal{D}_{i,m}}) \longrightarrow \gamma_i F_i(\pi_i) \quad \text{strongly in } L^2(\Gamma \times (0, t_f)).$$

F_i being increasing, we can reproduce the Minty trick of [19, Lemma D.10] to identify the limits and get $F_i(\pi_\Gamma) = \gamma_i F_i(\pi_i)$. This achieves the proof of the first transmission condition, namely (4.14). Let us now prove the second claim. We present the proof in the case of $\alpha = \mathrm{nw}$, a similar reasoning is conducted for $\alpha = \mathrm{w}$.

Let us define the following truncation function

$$T_i(u) = \begin{cases} \overline{\pi}_i & \text{if } u > \overline{\pi}_i \\ u & \text{if } \underline{\pi}_i \le u \le \overline{\pi}_i \\ \underline{\pi}_i & \text{if } u < \underline{\pi}_i. \end{cases}$$

We remark that $F_i' = 0$ outside $[\underline{\pi}_i, \overline{\pi}_i]$ and therefore $F_i \circ T_i = F_i$. Accordingly, $F_i\big(\pi_{\Gamma,\mathcal{D}_m}\big) = F_i\big(T_i(\pi_{\Gamma,\mathcal{D}_m})\big)$, which in view of Proposition 4.8 implies that

$$F_i\big(T_i(\pi_{\Gamma,\mathcal{D}_m})\big) \longrightarrow F_i\big(T_i(\pi_\Gamma)\big) \quad \text{a.e. in } \Gamma \times (0, t_f).$$

Since F_i is invertible on $[\underline{\pi}_i, \overline{\pi}_i]$ and its inverse function is continuous, it holds

$$T_i\big(\pi_{\Gamma,\mathcal{D}_m}\big) \longrightarrow T_i(\pi_\Gamma) \quad \text{a.e. in } \Gamma \times (0, t_f). \tag{4.16}$$

In order to prove (4.15) we remark that in view of (2.9) together with Assumptions $(\mathbf{A}_2)$ and $(\mathbf{A}_3)$, the function G_i^{nw} is identically zero on $(-\infty, \underline{\pi}_i)$ and is affine on $(\overline{\pi}_i, +\infty)$. We can write $G_i^{\mathrm{nw}}(u)$ in the following form

$$G_i^{\mathrm{nw}}(u) = G_i^{\mathrm{nw}}(T_i(u)) + \big(u - T_i(u)\big) f_i^{\mathrm{nw}}\Big(s_i(T_i(u))\Big).$$

In view of (4.13), (4.16) and using Lebesgue's dominate convergence theorem we deduce that

$$G_i^{\mathrm{nw}}(\pi_{\Gamma,\mathcal{D}_m}) \longrightarrow G_i^{\mathrm{nw}}(\pi_\Gamma) \quad \text{weakly in } L^2(\Gamma \times (0, t_f)),$$

which concludes the proof. □

It follows from Propositions 4.9 and 4.10 that the functions $(\pi_i, P_i)_{i\in\{1,2\}}$ satisfy the transmission conditions (2.16) and (2.17).

5 Numerical comparison of the PPU and HU TPFA schemes

The objective of this numerical section is to compare four different spatial discretizations in terms of accuracy and efficiency. Moreover, two different strategies to solve the nonlinear systems at each time step are also investigated either based on a local nonlinear interface solver or on a regularization of the interface system.

The first two spatial discretizations are both based on the classical Phase Potential Upwinding (PPU) discretization of transport terms combined with the TPFA discretization of the gradient fluxes. Two variants are considered, the first one denoted by **PPUI** uses interface unknowns at all interior faces $\sigma \in \mathcal{F}$ of the mesh and the second denoted by **PPU** uses interface unknowns only at faces $\sigma = K|L \in \mathcal{F}_\Gamma$ with heterogeneous rock types $\mathrm{rt}_K \neq \mathrm{rt}_L$. Let us refer e.g. to [37] for the cell-centered PPU discretization of multiphase Darcy flow and to [1] for a its extension to Discrete Fracture Matrix (DFM) models using interface unknowns at matrix fracture interfaces. The two other spatial discretizations are the ones described in this article based on the HU discretization of transport terms combined with the TPFA discretization of the gradient fluxes. Let us denote by **HUI** the discretization (3.3)-(3.7) with interface unknowns at all interior faces $\sigma \in \mathcal{F}$ and by **HU** the discretization with interface unknowns only at faces $\sigma \in \mathcal{F}_\Gamma$ with heterogeneous rock types as described in Subsection 3.3. Note that $c_{K,\sigma}$ in the total mobility (3.10) (and similarly $c_{K,L}$ in (3.18)) is approximated by $\frac{1}{2}(s_{\mathrm{rt}_K}(\pi_K^n) + s_{\mathrm{rt}_K}(\pi_\sigma^n))$ which amounts to use a one point quadrature formula. More advanced quadratures have been tested but they do not improve the accuracy and can reduce the efficiency of the nonlinear solver.

All these spatial discretizations are combined with a fully implicit Euler time discretization using the time stepping defined by $\Delta t^1 = \Delta t_{\mathrm{init}}$ and for all $n \geq 1$ by

$$\Delta t^{n+1} = \max(\Delta t_{\max}, 1.2\Delta t^n),$$

in case of a successful time step, and $\Delta t^{n+1} = \dfrac{\Delta t^n}{2}$, in case of non convergence of the Newton algorithm in $NL_{\max}$ iterations.

At each time step, the nonlinear system is solved using a Newton algorithm. Its convergence is improved by a suitable choice of the two primary unknowns. The first primary unknown is the non-wetting phase pressure at all cell and face degrees of freedom. For the second primary unknown, it is well known that the capillary pressure is not a robust choice. It is replaced by the non-wetting phase saturation at all cells and, for the HUI and PPUI schemes, at all faces $\sigma \in \mathcal{F}_1 \cup \mathcal{F}_2$ with homogeneous rock types. For faces $\sigma \in \mathcal{F}_\Gamma$ with heterogeneous rock types, a switch of variable parametrization of the capillary pressure monotone graphs is used as second primary unknown as introduced in [9]. We would like to indicate that some alternative linearization schemes to Newton's method devoted to the improvement of the nonlinear solver have been proposed in [36, 38, 40].

To further improve the nonlinear convergence, two different strategies are compared to update the face unknowns in the present work. The first technique combines the regularization presented in (3.15) with a linear Newton update of the face unknowns. The second technique updates the face unknowns by solving the local nonlinear system on each face. For the HU and HUI discretizations, this local system is defined by (3.23) and solved by explicit elimination of the non-wetting phase pressure followed by a dichotomy on π_σ. For the PPU and PPUI schemes, the algorithm to solve the local interface system is detailed in [1]. In Subsection 5.2, we denote by "-is" the nonlinear update using the interface local nonlinear solver and by "-vol" the regularization combined with linear Newton update of the face unknowns.

In all cases, the interface unknowns are eliminated without any fill-in before solving the Jacobian linear system. Then a GMRes iterative algorithm preconditioned by the CPR-AMG preconditioner [35, 42] is applied on the reduced Jacobian. To obtain a more robust convergence of the nonlinear solver, a damping of the Newton step is applied enforcing a prescribed maximum variation of the saturation. This strategy is applied for all test cases and all schemes. The GMRes stopping criterion on the relative residual is fixed to 10^{-6}. The Newton solver is convergent if the relative residual is lower than 10^{-5} or if the weighted maximum norm of the Newton increment is lower than 10^{-4}. We denote by $N_{\triangle t}$ the number of successful time steps, by $N_{\rm Chop}$ the number of time step chops, by $N_{\rm Newton}$ the average number of Newton iterations per successful time step, and by $N_{\rm GMRes}$ the average number of GMRes iterations per Newton iteration. Finally, CPU (s) stands for the CPU time in seconds.

5.1 Oil migration in a 1D basin with capillary barrier

We consider the vertical 1D basin domain $\Omega = (0, L_z)$ with $L_z = 800\ m$ including a drain rock type on $\Omega_2 = (0, \frac{L_z}{2})$ and a barrier rocktype on $\Omega_1 = \Omega \setminus \overline{\Omega}_2$.

The drain and barrier subdomains have the same porosity $\phi = 0.2$, permeability $\Lambda = 10^{-13}$ m^2, and relative permeabilities given by $k_r^\alpha(s^\alpha) = (s^\alpha)^2$, $\alpha = nw, w$. The capillary pressure is fixed to

$$P_{c,1}(s^{\rm nw}) = 6.10^5 + 10^3\ s^{\rm nw}\ \text{Pa}$$

in the barrier, and to

$$P_{c,2}(s^{\rm nw}) = 10^3\ s^{\rm nw}\ \text{Pa}$$

in the drain. The fluid properties are defined by their dynamic viscosities $\mu^{\rm nw} = 5.\ 10^{-3}$, $\mu^{\rm w} = 10^{-3}$ Pa.s and their mass densities $\rho^{\rm w} = 1000$ and $\rho^{\rm nw} = 700$ Kg.m^{-3}.

Note that the permeability and porosity are chosen homogeneous for this test case in order to emphasize the capillary barrier effect at the interface between the drain and barrier subdomains. The basin is initially saturated by water and the oil phase is injected at the bottom boundary $z = 0$ using the Dirichlet input boundary condition $s^{\rm nw} = 0.5$ on the time interval $t \in [0, t_1]$. For $t \in [t_1, t_f]$ the input Dirichlet boundary condition is changed to $s^{\rm nw} = 0$, with $t_1 = 400$ years and $t_f = 800$ years. The pressure is fixed to $p^{\rm nw} = 8.1\ 10^6$ Pa at $z = 0$ and to $p^{\rm w} = 10^5$ Pa at $z = L_z$. The oil phase rises by gravity untill it reaches a stationary state corresponding to the trapping of the oil phase in the drain.

From Figures 3-4-5 one can check on the coarse mesh $n_z = 20$ that the TPFA HU scheme is more diffusive than the TPFA PPU scheme although both schemes capture in an excellent way the saturation jump at the interface between both rock types thanks to the interface degree of freedom. This additional diffusion of the HU scheme compared with the PPU scheme was expected for dominant gravity and capillary effect compared with viscous forces. On the other hand, the HUI version removes most of this additional diffusion of the HU scheme thanks to the additional interface unknowns at homogeneous interfaces. We also remark that the four schemes provide very close solutions on the fine mesh with $n_z = 200$.

The numerical performance of the nonlinear solver is exhibited on Figure 6 using a coarse time stepping defined by $\Delta t_{\text{init}} = 1$ year and $\Delta t_{\max} = 10$ years on the fine mesh $n_z = 800$. For all schemes, the interface unknowns are updated at each Newton iteration using an interface local nonlinear solver. It is clearly seen that the TPFA HU and HUI schemes are more efficient than the TPFA PPU and PPUI schemes.

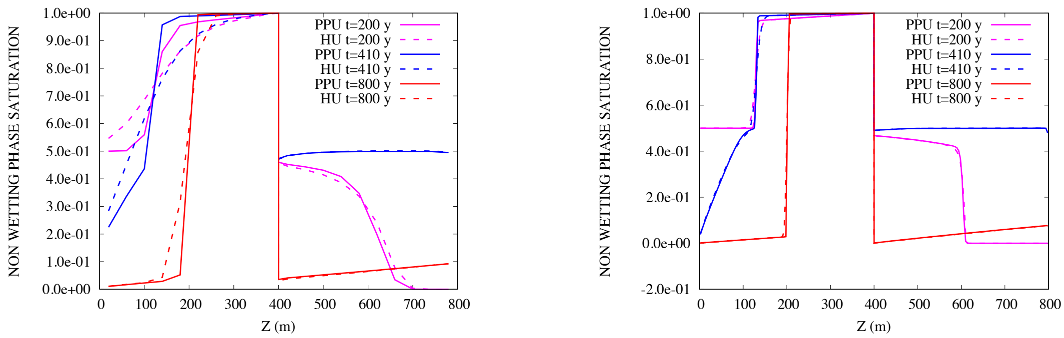

Figure 3: Non-wetting phase saturations as a function of z at different times $t = 200, 410, 800$ years, obtained for the TPFA PPU and HU schemes on the 20 cells (left) and 200 cells (right) meshes.

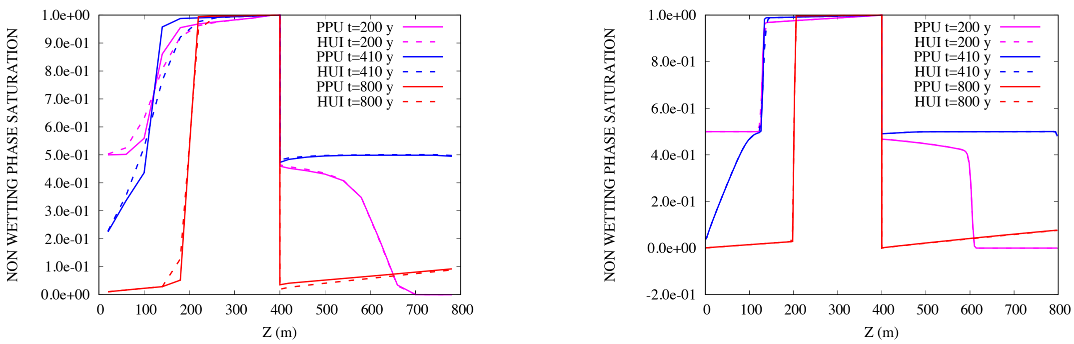

Figure 4: Non-wetting phase saturations as a function of z at different times $t = 200, 410, 800$ years, obtained for the TPFA PPU and HUI schemes on the 20 cells (left) and 200 cells (right) meshes.

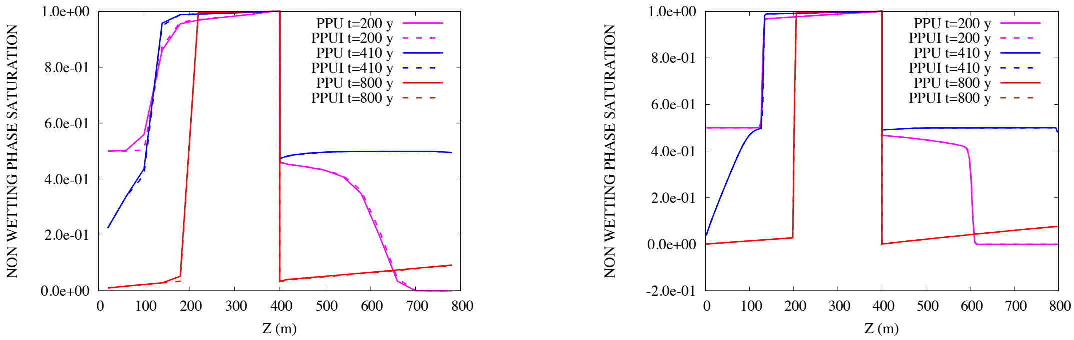

Figure 5: Non-wetting phase saturations as a function of z at different times $t = 200, 410, 800$ years, obtained for the TPFA PPU and PPUI schemes on the 20 cells (left) and 200 cells (right) meshes.

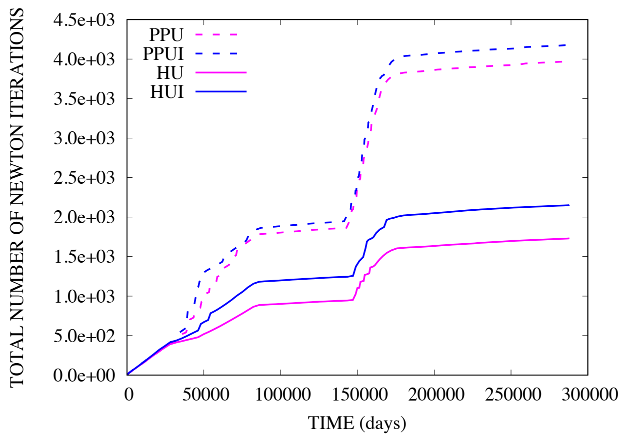

Figure 6: Accumulated number of Newton iterations as a function of time on $(0, t_f)$ with $t_f = 800$ years for the TPFA HU, PPU, HUI, PPUI schemes on the 800 cells mesh with large time steps.

5.2 Oil migration in a 2D large DFM model

The objective of the next test case is to compare the efficiency in terms of nonlinear convergence and CPU time of the TPFA PPU and HUI schemes (which essentially have the same accuracy). The test case considers the Discrete Fracture Matrix (DFM) model with the matrix domain $\Omega = (0, L) \times (0, H)$, $L = 100$ m, $H = 186.5$ m, and a fracture network including 581 connected components; see Figure 7. The fracture width is $d_f = 10^{-3}$ m and the fracture network is homogeneous and isotropic with $\Lambda_f = 10^{-7}$ m^2, $\phi_f = 0.2$. The matrix is homogeneous and isotropic with $\Lambda_m = 10^{-13}$ m^2, $\phi_m = 0.35$. The matrix and the fracture network have the same relative permeabilities given by $k^\alpha_{r,f}(s^\alpha) = k^\alpha_{r,m}(s^\alpha) = (s^\alpha)^2$, $\alpha \in \{\mathrm{nw}, \mathrm{w}\}$, and the capillary pressure is fixed to

$$P_{c,m}(s^{\mathrm{nw}}) = 10^5(1 - \log(1 - s^{\mathrm{nw}}))\ \mathrm{Pa}$$

in the matrix, and to

$$P_{c,f}(s^{\mathrm{nw}}) = -100 \log(1 - s^{\mathrm{nw}})\ \mathrm{Pa}$$

in the fracture network. The fluid properties are defined by their dynamic viscosities $\mu^{\mathrm{nw}} = 5.\ 10^{-3}$, $\mu^{\mathrm{w}} = 10^{-3}$ Pa.s and their mass densities $\rho^{\mathrm{w}} = 1000$ and $\rho^{\mathrm{nw}} = 800$ Kg.m^{-3}.

The reservoir is initially saturated with water. Dirichlet boundary conditions are imposed at the top boundary with zero water pressure and non-water saturation, as well as at the bottom boundary with $s_m^{\mathrm{nw}} = 0.9$ and $p_m^{\mathrm{w}} = \rho^{\mathrm{w}} g H$. The remaining boundaries are assumed impervious and the final simulation time is fixed to $t_f = 360$ days. The time stepping is defined by $\Delta t^1 = \Delta t_{\mathrm{init}} = 1$ day, $\Delta t_{\max} = 1$ day, and by $NL_{\max} = 50$ iterations.

Table 1 reports the number of d.o.f. (with two physical primary unknowns per d.o.f.) before reduction (N) and after reduction (N_{red}), as well as the number of nonzero element in the Jacobian (with 2×2 elements) before reduction (NZ) and after reduction (NZ_{red}).

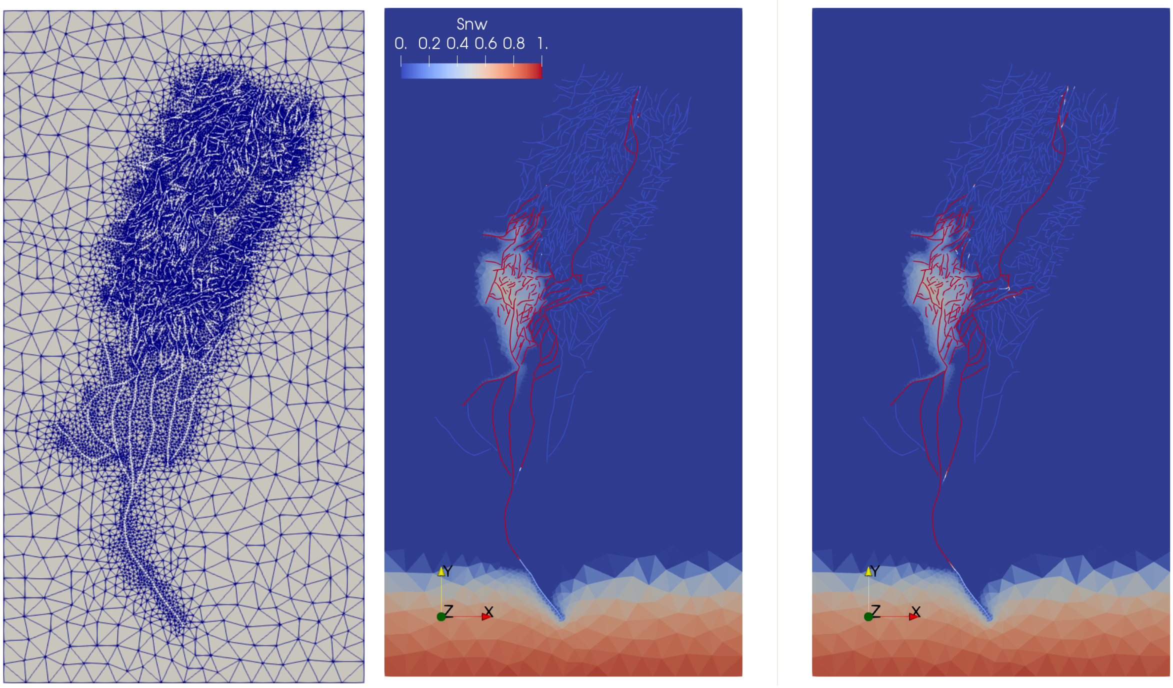

Figure 7: Left: triangular mesh of the DFM model with 32340 cells, 48558 faces and 5344 fracture faces (Courtesy of M. Karimi-Fard, Stanford, and A. Lapène, Total). Non-wetting phase saturation at final simulation time for the TPFA PPU (middle) and HUI (right) schemes.

The non-wetting phase saturation solution at final time is exhibited in Figure 7 in the matrix and in the fracture network. Figure 8 plots the matrix and fracture non-wetting phase volumes as a function of time. Both figures clearly show that the TPFA PPU and HUI schemes provide very close solutions.

It is clear from Table 2 and Figure 9 that the regularization combined with linear Newton update is more efficient than the implementation with zero volumes and interface local solver. Moreover, considering the same implementation, the TPFA HUI scheme is much more efficient than the TPFA PPU scheme. The regularization parameter ϵ in (3.15) is fixed to 10^{-2} at cell-cell interfaces and to 10^{-1} at cell-fracture face interfaces. Note that there is no significant differences between the solution obtained with this regularization and the one obtained with the interface solver using $\epsilon = 0$.

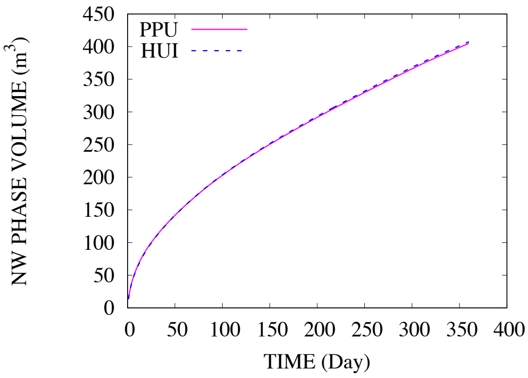

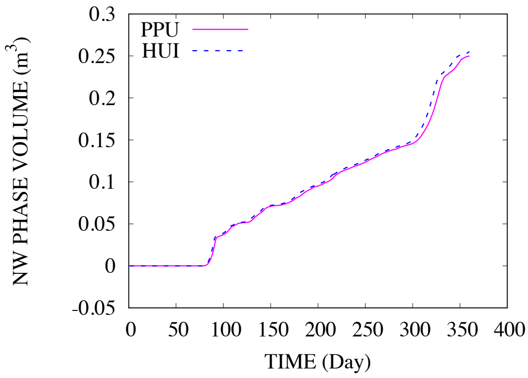

Figure 8: Volume of the non-wetting phase in the matrix (left) and in the fractures (right) as a function of time for the TPFA PPU and HUI schemes.

scheme	N	NZ	N_{red}	NZ_{red}
PPU	48400	208380	37712	154940
HUI	91518	423970	37712	154940

Table 1: Number of d.o.f. of the discretization (N and N_{red}) and number of nonzero elements in the Jacobian (NZ and NZ_{red}) before and after reduction.

scheme	$N_{\triangle t}$	N_{Chop}	N_{Newton}	N_{GMRes}	CPU(s)
PPU-is	x	x	x	x	x
HUI-is	444	42	22.1	47	7350
PPU-vol	399	19	23.8	47	6504
HUI-vol	364	3	14.8	49	3910

Table 2: Numerical behavior of the simulation for the large 2D DFM test case using the TPFA PPU and HUI schemes combined with an interface nonlinear solver (is) or with the regularization (3.15) at the interface and linear Newton update (vol).

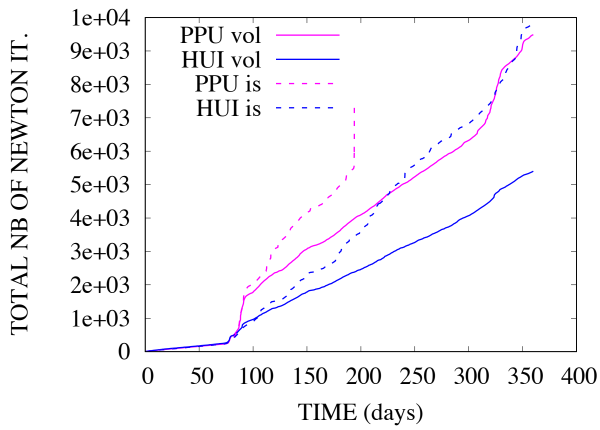

Figure 9: Accumulated number of Newton iterations as a function of time on $(0, t_f)$ for the TPFA HUI and PPU schemes combined (is) or not (vol) with an interface nonlinear solver.

6 Conclusions

A fully implicit Two-Point Flux Approximation (TPFA) based on the total velocity formulation and a Hybrid Upwinding (HU) approximation of the transport term is proposed. It incorporates cell centered as well as face centered unknowns enabling the accurate capture of the nonlinear transmission conditions at different rocktype interfaces. It is based on natural physical unknowns avoiding the cumbersome use in the scheme's design of the global pressure and of the Kirchhoff transform. Energy estimates on the global pressure are recovered thanks to a specific centered approximation of the phase mobilities in the definition of the total velocity. This plays a key role in the convergence proof of the scheme to a weak solution; this proof is based on relative compactness estimates and on the convergence of traces at different rock type interfaces.

Numerical experiments compare the proposed TPFA HU scheme to the classical TPFA Phase Potential Upwinding (PPU) scheme both in terms of accuracy and efficiency on two test cases including a highly heterogeneous Discrete Fracture Matrix model. Thanks to the face unknowns incorporated in the discretization for both schemes, the numerical results exhibit comparable accuracy of both HU and PPU schemes combined with an additional robustness and a significant gain in CPU time. For both the TPFA HU and PPU schemes, it is also shown that the regularization strategy at different rock type interfaces based on an additional small accumulation term combined with a Newton linear update of the interface unknowns performs better than the nonlinear update of these interface unknowns based on a local nonlinear interface solver. In all cases, the face unknowns are eliminated from the Jacobian system by Schur complement leading, roughly speaking, to the same complexity as a cell-centered TPFA discretization.

Acknowledgments

The authors would like to thank the French National Research Agency for its support in the framework of the CHARMS ANR project ANR-16-CE06-0009, and to the Australian Research Council's Discovery Projects (project DP170100605) funding scheme for partially supporting this work.

References

[1] J. Aghili, K. Brenner, J. Hennicker, R. Masson, and L. Trenty. Two-phase Discrete Fracture Matrix models with linear and nonlinear transmission conditions. *GEM – International Journal on Geomathematics*, 10, 2019.

[2] E. Ahmed, S. A. Hassan, C. Japhet, M. Kern, and M. Vohralík. A posteriori error estimates and stopping criteria for space-time domain decomposition for two-phase flow between different rock types. *The SMAI Journal of Computational Mathematics*, 5:195–227, 2019.

[3] A. H. Alali, F. P. Hamon, B. P. Mallison, and H. A. Tchelepi. Finite-Volume Simulation of Capillary-Dominated Flow in Matrix-Fracture Systems using Interface Conditions. *Computational Geosciences*, 25:17–33, 2021.

[4] J. Bear and Y. Bachmat. *Introduction to Modeling of Transport Phenomena in Porous Media*, volume 4 of *Theory and Applications of Transport in Porous Media*. Kluwer Academic Publishers, Dordrecht, Holland, 1990.

[5] I. Bogdanov, V. Mourzenko, J.-F. Thovert, and P. Adler. Two-phase flow through fractured porous media. *Physical Review E*, 68(2):026703, 2003.

[6] Y. Brenier and J. Jaffré. Upstream differencing for multiphase flow in reservoir simulation. *SIAM Journal on Numerical Analysis*, 28(3):685–696, 1991.

[7] K. Brenner, C. Cancès, and D. Hilhorst. Finite volume approximation for an immiscible two-phase flow in porous media with discontinuous capillary pressure. *Computational Geosciences*, 17(3):573–597, 2013.

[8] K. Brenner, M. Groza, C. Guichard, and R. Masson. Vertex approximate gradient scheme for hybrid dimensional two-phase Darcy flows in fractured porous media. *ESAIM: Mathematical Modelling and Numerical Analysis*, 49(2):303–330, 2015.

[9] K. Brenner, M. Groza, L. Jeannin, R. Masson, and J. Pellerin. Immiscible two-phase Darcy flow model accounting for vanishing and discontinuous capillary pressures: application to the flow in fractured porous media. *Computational Geosciences*, 21(5):1075–1094, Dec 2017.

[10] K. Brenner, R. Masson, and E. H. Quenjel. Vertex Approximate Gradient Discretization preserving positivity for two-phase Darcy flows in heterogeneous porous media. *Journal of Computational Physics*, 409:109357, 2020.

[11] C. Cancès. Finite volume scheme for two-phase flows in heterogeneous porous media involving capillary pressure discontinuities. *Mathematical Modelling and Numerical Analysis*, 43:973–1001, 2009.

[12] C. Cancès and M. Pierre. An existence result for multidimensional immiscible two-phase flows with discontinuous capillary pressure field. *SIAM J. Math. Anal.*, 44:966–992, 2012.

[13] G. Chavent and J. Jaffré. *Mathematical models and finite elements for reservoir simulation: single phase, multiphase and multicomponent flows through porous media*, volume 17. North-Holland, Amsterdam, Stud. Math. Appl. edition, 1986.

[14] Z. Chen and R. E. Ewing. Fully discrete finite element analysis of multiphase flow in groundwater hydrology. *SIAM journal on numerical analysis*, 34(6):2228–2253, 1997.

[15] Z. Chen and R. E. Ewing. Degenerate two-phase incompressible flow III. Sharp error estimates. *Numerische Mathematik*, 90(2):215–240, 2001.

[16] K. Deimling. *Nonlinear functional analysis*. Springer-Verlag, Berlin, 1985.

[17] B. Doyle, B. Riviere, and M. Sekachev. A multinumerics scheme for incompressible two-phase flow. *Computer Methods in Applied Mechanics and Engineering*, 370:113213, 2020.

[18] J. Droniou and R. Eymard. The asymmetric gradient discretisation method. In *International Conference on Finite Volumes for Complex Applications VIII- methods and theoretical aspects*, volume 199 of Springer Proc. Math. Stat., pages 311–319. Springer, 2017.

[19] J. Droniou, R. Eymard, T. Gallouët, C. Guichard, and R. Herbin. *The gradient discretisation method*, volume 82 of *Mathematics & Applications*. Springer, 2018.

[20] J. Droniou, J. Hennicker, and R. Masson. Numerical analysis of a two-phase flow discrete fracture model. *Numerische Mathematik*, 141(1):21–62, 2019.

[21] G. Enchéry, R. Eymard, and A. Michel. Numerical approximation of a two-phase flow problem in a porous medium with discontinuous capillary forces. *SIAM Journal on Numerical Analysis*, 43(6):2402–2422, 2006.

[22] G. Enchéry, R. Masson, S. Wolf, and R. Eymard. Mathematical and numerical study of an industrial scheme for two-phase flows in porous media under gravity. *Computational Methods in Applied Mathematics*, 2(4):325–353, 2002.

[23] A. Ern, I. Mozolevski, and L. Schuh. Discontinuous Galerkin approximation of two-phase flows in heterogeneous porous media with discontinuous capillary pressures. *Computer Methods in Applied Mechanics and Engineering*, 199(23-24):1491–1501, 2010.

[24] R. Eymard, T. Gallouët, and R. Herbin. Discretization of heterogeneous and anisotropic diffusion problems on general nonconforming meshes sushi: a scheme using stabilization and hybrid interfaces. *IMA Journal of Numerical Analysis*, 30(4):1009–1043, 2010.

[25] R. Eymard, T. Gallouët, and P. Joly. Hybrid Finite Element Techniques for Oil Recovery Simulation. *Computer Methods in Applied Mechanics and Engineering*, 74, 1989.

[26] R. Eymard, C. Guichard, R. Herbin, and R. Masson. Gradient schemes for two-phase flow in heterogeneous porous media and richards equation. *ZAMM-Journal of Applied Mathematics and Mechanics/Zeitschrift für Angewandte Mathematik und Mechanik*, 94(7-8):560–585, 2014.

[27] R. Eymard, R. Herbin, and A. Michel. Mathematical study of a petroleum-engineering scheme. *ESAIM: Mathematical Modelling and Numerical Analysis*, 37(6):937–972, 2003.

[28] T. Gallouët and A. Pfertzel. On some upstream weighting schemes for oil recovery simulation. *Les Annales de l'Enit*, 4(2), 1990.

[29] D. Gläser, R. Helmig, B. Flemisch, and H. Class. A discrete fracture model for two-phase flow in fractured porous media. *Advances in Water Resources*, 110:335–348, 2017.

[30] F. P. Hamon, B. T. Mallison, and H. A. Tchelepi. Implicit Hybrid Upwind scheme for coupled multiphase flow and transport with buoyancy. *Computer Methods in Applied Mechanics and Engineering*, 311:599–624, 2016.

[31] F. P. Hamon, B. T. Mallison, and H. A. Tchelepi. Implicit hybrid upwinding for two-phase flow in heterogeneous porous media with buoyancy and capillarity. *Computer Methods in Applied Mechanics and Engineering*, 331:701–727, 2018.

[32] R. Helmig. *Multiphase flow and transport processes in the subsurface: a contribution to the modeling of hydrosystems.* Springer-Verlag, 1997.

[33] C. K. Ho and S. W. Webb. Capillary barrier performance in heterogeneous porous media. *Water Resources Research*, 34(4):603–609, 1998.

[34] H. Hoteit and A. Firoozabadi. An efficient numerical model for incompressible two-phase flow in fractured media. *Advances in Water Resources*, 31(6):891–905, 2008.

[35] S. Lacroix, Y. V. Vassilevski, and M. F. Wheeler. Decoupling preconditioners in the implicit parallel accurate reservoir simulator (IPARS). *Numerical Linear Algebra with Applications*, 8(8):537–549, dec 2001.

[36] K. Mitra and I. S. Pop. A modified L-scheme to solve nonlinear diffusion problems. *Computers & Mathematics with Applications*, 77(6):1722–1738, 2019.

[37] D. W. Peaceman. *Fundamentals of numerical reservoir simulation.* Elsevier, 2000.

[38] I. S. Pop, F. Radu, and P. Knabner. Mixed finite elements for the Richards' equation: linearization procedure. *Journal of Computational and Applied Mathematics*, 168(1-2):365–373, 2004.

[39] F. A. Radu, K. Kumar, J. M. Nordbotten, and I. S. Pop. A robust, mass conservative scheme for two-phase flow in porous media including hölder continuous nonlinearities. *IMA Journal of Numerical Analysis*, 38(2):884–920, 2018.

[40] F. A. Radu, J. M. Nordbotten, I. S. Pop, and K. Kumar. A robust linearization scheme for finite volume based discretizations for simulation of two-phase flow in porous media. *Journal of Computational and Applied Mathematics*, 289:134–141, 2015.

[41] V. Reichenberger, H. Jakobs, P. Bastian, and R. Helmig. A mixed-dimensional finite volume method for two-phase flow in fractured porous media. *Advances in Water Resources*, 29(7):1020–1036, 2006.

[42] R. Scheichl, R. Masson, and J. Wendebourg. Decoupling and block preconditioning for sedimentary basin simulations. *Computational Geosciences*, 7(4):295–318, 2003.

[43] J. C. Stormont and C. E. Anderson. Capillary barrier effect from underlying coarser soil layer. *Journal of Geotechnical and Geoenvironmental Engineering*, 125(8):641–648, 1999.

[44] C. J. Van Duijn, J. Molenaar, and M. De Neef. The effect of capillary forces on immiscible two-phase flow in heterogeneous porous media. *Transport in Porous Media*, 21(1):71–93, 1995.